

PHILIPP TSCHANN

# Emission and Performance Studies of Alternative Fuels

Supervised by

Univ.-Prof. Dr. Helmut EICHLSEDER

Institute for Internal Combustion Engines and Thermodynamics  
Graz University of Technology, Austria

Professor Robert W. DIBBLE

Department of Mechanical Engineering  
University of California at Berkeley, USA

A diploma thesis submitted to the  
FACULTY OF MECHANICAL ENGINEERING AND ECONOMIC STUDIES  
GRAZ UNIVERSITY OF TECHNOLOGY

October 2009



## **STATUTORY DECLARATION**

I declare that I have authored this thesis independently, that I have not used other than the declared sources/resources, and that I have explicitly marked all material which has been quoted either literally or by content from the used sources.

Date \_\_\_\_\_

Signature: \_\_\_\_\_

## **EIDESSTATTLICHE ERKLÄRUNG**

Ich erkläre an Eides statt, dass ich die vorliegende Arbeit selbstständig verfasst, andere als die angegebenen Quellen/Hilfsmittel nicht benutzt, und die den benutzten Quellen wörtlich und inhaltlich entnommenen Stellen als solche kenntlich gemacht habe.

Graz, am \_\_\_\_\_

Unterschrift: \_\_\_\_\_



## **Acknowledgements**

This thesis is the product of the work and support of many people and I am extremely grateful to all who have had an influence throughout the years.

Firstly, I would like to express my gratitude to my advisor at Graz University of Technology, Univ.–Prof. Dr. Helmut Eichlseder, who kindly tutored this thesis and enabled me to write my thesis abroad. I would also like to thank Dr. Peter Grabner for his help in the final stage of this thesis.

My advisor at University of California at Berkeley, Professor Robert W. Dibble, who kindly accepted me as his student, tutored my thesis and provided me with great scientific but also personal guidance. Furthermore, I would like to thank MaryAnne Peters for her help in various ways as well as the mechanical service group in Hesse Hall including Scott McCormick, Mike Neuffer, Pete Graham and Alex Jordan.

I would also like to thank my lab mates Vi Rapp, Andrew Van Blarigan, Wolfgang Hable, Dr. Hunter Mack and Dr. Nick Killingsworth for the many hours we spent on the experiments, for the fruitful discussions we had and for creating such a friendly environment.

I am very grateful for the financial support by the Austrian Marshallplan Scholarship as well as the Hans List Stipendium for providing funding for this thesis.

Finally, my most profound thanks go to my parents Gabriele and Anton for the support they gave me and always having faith in me.



## Abstract

An experimental study of emissions and performance of a mixture of alcohols (ethanol, propanol, butanol, pentanol) was conducted in a single cylinder cooperative fuel research engine (CFR), the standard engine for octane rating. Particularly ethanol has proven itself as a blending agent but little research has been conducted or published for higher alcohols. The alcohols used in this thesis derive from a thermochemical conversion of biomass to alcohols, thus produced in a rather sustainable way.

The so-called MixedAlcohol blend, with ethanol being the main component (75%), was used as a blending agent in non-oxygenated gasoline, so-called Carbob. MixedAlcohol/Carbob blends in the level of 5%, 10%, 15% and 85% as well as neat Carbob and MixedAlcohol were tested and compared against each other.

Typically, cylinder pressure was recorded with an encoder resolution of 0.1 crank angle degree. An indicating number (*IMPO*) was calculated from the band-pass filtered cylinder pressure data followed by an integration over a certain window in crank angle degrees. The knock intensity was determined by a comparison of the *IMPO* with a defined critical *IMPO*.

Octane numbers were determined with a procedure adapted to the research octane method (RON). An almost linear relation between the carbon number of alcohols and the octane number was found. For all MixedAlcohol blends an increase in octane number with increasing MixedAlcohol content could be found. For the neat MixedAlcohol blend an octane number of approximately 110 was determined.

Performance tests were conducted at 900 rpm, stoichiometric air/fuel ratio and wide open throttle. A compression ratio sweep as well as a spark timing sweep was conducted in order to find the combination producing the highest *IMEP*. The MixedAlcohol blend proved its ability to increase the *IMEP* with increasing blending level. The neat MixedAlcohol blend showed an increase in *IMEP* relative to Carbob of 21%.

Cycle emissions (*ppm*) of unburnt hydrocarbons increased with higher MixedAlcohol content. Cycle emissions of CO showed a significant reduction for the high level blends, with more than 20% for the 85% blend. In terms of  $\text{NO}_x$  cycle emissions no real trend could be found. Brake specific emissions (*ppm/kW*) of CO and  $\text{NO}_x$  showed a progressive reduction with increasing blending level.





## Zusammenfassung

Ein noch nicht erforschtes Gemisch aus Alkoholen (Ethanol, Propanol, Butanol, Pentanol), sogenannte Biokraftstoffe der zweiten Generation, wurden in einem Einzylinder-Forschungsmotor mit variablem Verdichtungsverhältnis bezüglich Leistung und Emissionen getestet. Vor allem Ethanol hat sich bereits als Zusatz zu Benzin bewährt, während höherwertige Alkohole bisher kaum verwendet werden und noch relativ wenig Forschungsarbeit geleistet wurde.

Das Alkohol-Gemisch, hier als MixedAlcohol bezeichnet, in dem Ethanol mit 75% den Hauptbestandteil ausmacht, wurde als Komponente für Mischungen mit sauerstofffreiem Benzin, hier Carbob genannt, verwendet. MixedAlcohol/Carbob-Gemische in volumetrischen Mischungsverhältnissen von 5%, 10%, 15% und 85% sowie MixedAlcohol und Carbob selbst wurden getestet und verglichen.

Eine Bewertung des Klopfens wurde mittels Druckverlaufsanalyse durchgeführt. Aus dem band-pass gefilterten Druckverlauf wurde eine charakteristische Größe berechnet (*IMPO*) und im Vergleich mit einem definierten kritischen *IMPO* wurde die Klopfintensität bestimmt.

Die Oktanzahlen wurden mittels einer an den Standard angelehnten aber neu entwickelten Methode bestimmt. Für höherwertige Alkohole konnte ein linearer Zusammenhang zwischen der Oktanzahl und der Anzahl der Kohlenstoffatome gefunden werden. Bei den MixedAlcohol/Carbob-Gemischen wurde ein regressiver Zusammenhang festgestellt wobei für das MixedAlcohol-Gemisch eine Oktanzahl von etwa 110 bestimmt wurde.

Die Leistung jedes Gemisches wurde bei einer Motordrehzahl von 900 1/min, unter Volllast und bei stöchiometrischem Betrieb bestimmt. Durch gleichzeitiges Verändern des Verdichtungsverhältnisses sowie des Zündzeitpunktes wurde die Kombination mit dem höchsten indizierten Mitteldruck bestimmt. Eine Beimischung von MixedAlcohol bewirkte immer eine Leistungssteigerung wobei ein Leistungsunterschied zwischen Carbob und MixedAlcohol von 21% festgestellt wurde.

In allen MixedAlcohol-Gemischen wurden höhere HC-Emissionen (*ppm*) gemessen als mit Carbob. Bei den CO-Emissionen konnte eine deutliche Reduktion (bis zu 20%) bei hohem MixedAlcohol-Anteil festgestellt werden. Bei den Stickoxid Emissionen wurde kein eindeutiger Trend festgestellt. Die höhere Leistung des MixedAlcohol Gemisches bewirkte jedoch eine progressive Verringerung der spezifischen  $\text{NO}_x$ - und CO-Emissionen (*ppm/kW*).



# Contents

<b>List of Figures</b>	<b>xv</b>
<b>List of Tables</b>	<b>xvii</b>
<b>1. Introduction</b>	<b>1</b>
1.1. The Project . . . . .	2
1.2. Biofuels . . . . .	3
1.3. Thesis Overview . . . . .	4
<b>2. Fuel Chemistry</b>	<b>7</b>
2.1. Hydrocarbons . . . . .	7
2.1.1. Alkanes (Paraffins) . . . . .	8
2.1.2. Cycloalkanes (Naphthenes) . . . . .	10
2.1.3. Alkenes (Olefine) . . . . .	11
2.1.4. Aromatic Hydrocarbon . . . . .	11
2.2. Oxygenated Hydrocarbons . . . . .	11
2.2.1. Alcohols . . . . .	11
2.2.2. Ether . . . . .	15
2.3. Additives . . . . .	15
<b>3. Combustion</b>	<b>17</b>
3.1. Stoichiometric Air Requirement . . . . .	17
3.2. Normal Combustion . . . . .	18
3.2.1. Thermal Ignition – Ignition Process . . . . .	18
3.2.2. Autoignition – Ignition Limits . . . . .	20
3.2.3. Autoignition – Ignition Delay Time . . . . .	21
3.2.4. Detonation . . . . .	21
3.3. Abnormal Combustion . . . . .	21
3.3.1. Surface Ignition . . . . .	22
3.3.2. Engine Knock . . . . .	22

3.4.	Formation of Pollutants . . . . .	24
3.4.1.	Nitrogen Oxide Formation . . . . .	24
3.4.2.	Hydrocarbon and Soot Formation . . . . .	26
<b>4.</b>	<b>Experimental Setup</b>	<b>27</b>
4.1.	Cooperative Fuel Research Engine (CFR) . . . . .	27
4.1.1.	Differences between the CFR F1/F2 model and the CFR F4 model . . .	29
4.1.2.	Engine upgrade . . . . .	33
4.2.	Measurement System . . . . .	34
4.2.1.	In-Cylinder Pressure Measurement . . . . .	34
4.3.	Data Acquisition (DAQ) . . . . .	35
4.4.	Emission Measurement . . . . .	36
<b>5.</b>	<b>Experimental Procedure</b>	<b>39</b>
5.1.	Fuels . . . . .	39
5.2.	Research Octane Number (RON) . . . . .	40
5.2.1.	The ASTM D 2699 Standard Test Method for Research Octane Number of Spark-Ignition Engine Fuels. . . . .	41
5.2.2.	The Applied Procedure . . . . .	43
5.3.	Performance Tests . . . . .	45
5.4.	Emission Tests . . . . .	46
<b>6.</b>	<b>Analysis Methods</b>	<b>47</b>
6.1.	Overview of Knock Detection Methods . . . . .	47
6.2.	Used Knock Detection Methods . . . . .	52
6.3.	Determination of Octane Number . . . . .	53
6.4.	Performance Analysis . . . . .	54
6.4.1.	Indicated Mean Effective Pressure (IMEP) . . . . .	54
6.4.2.	Heat Release . . . . .	55
6.4.3.	Mass fraction Burnt Analysis . . . . .	56
6.4.4.	Gas Temperature . . . . .	58
6.5.	Emissions analyses . . . . .	59
<b>7.</b>	<b>Results</b>	<b>61</b>
7.1.	Determined Octane Number . . . . .	61
7.2.	Performance Tests . . . . .	63
7.2.1.	Exhaust Gas and Burnt Gas Temperature . . . . .	67
7.2.2.	Net Heat Release Rate Analysis – Mass Fraction Burnt Analysis . . . .	68
7.3.	Emission Tests . . . . .	71

<b>8. Conclusions and Future Work</b>	<b>77</b>
8.1. Conclusion . . . . .	77
8.2. Future Work . . . . .	78
<b>Bibliography</b>	<b>79</b>
<b>List of Symbols</b>	<b>83</b>
<b>A. Calculations</b>	<b>87</b>
<b>B. Chemical Properties of Alcohols</b>	<b>91</b>
<b>C. Determination of Knock Limiting Compression Ratio</b>	<b>93</b>



# List of Figures

1.1. Schematic view of the thermochemical conversion of carbon in biomass to a MixedAlcohol liquid fuel. . . . .	2
2.1. n-Heptane ( $C_7H_{16}$ ) and 2,2,4 Trimethylpentane ( $C_8H_{18}$ ). . . . .	8
2.2. Time to autoignition as a function of temperature and carbon monoxide concentration as a function of compression ratio. . . . .	10
2.3. Benzene ( $C_6H_6$ ) and Methylbenzene ( $C_6H_5CH_3$ ). . . . .	11
2.4. Comparison in boiling points of alkanes and boiling points of alcohols. . . . .	14
2.5. Lower heating value (LHV) of different fuels and lower heating value of stoichiometric air/fuel mixtures ( $LHV_m$ ). . . . .	15
3.1. Schematic illustration of the temperature dependences of heat production and heat losses. . . . .	19
3.2. Ignition limits for hydrocarbons. . . . .	20
4.1. Schematic view of the CFR test bench. . . . .	28
4.2. Cross-sectional view of a CFR F1/F2 model. . . . .	30
4.3. Comparison of intake valves between different CFR models. . . . .	32
4.4. Calculated frequencies for the used pressure transducer setup. . . . .	35
4.5. Operating Principles of the Hydrogen Flame Ionization Detector. . . . .	36
4.6. AIA measurement – Infrared Analyzer. . . . .	37
5.1. Characteristics of performance at different compression ratios. . . . .	45
6.1. Pressure oscillations in a knocking cycle. . . . .	48
6.2. Maximum amplitude of pressure oscillation under different operating conditions. . . . .	49
6.3. Pressure trace and third derivative of two different cycles . . . . .	51
6.4. Sketch of <i>IMPO</i> determination. . . . .	52
6.5. Knock frequency analysis of a knocking operating point. . . . .	53
6.6. Behaviour of the <i>IMPO</i> over compression ratio. . . . .	54
6.7. Exceed in <i>IMPO</i> limit and critical compression ratios (CRC). . . . .	55
6.8. Net heat release rate $dQ_{net}/d\theta$ and cumulative net heat release rate $Q_{cum}$ . . . . .	56

6.9. Measured pressure change as a sum of piston motion and combustion. . . . .	58
7.1. Dependence of determined octane number DON on number of carbon atoms. . .	62
7.2. Determined octane number of different MixedAlcohol blends. . . . .	63
7.3. Increase in knock limiting compression ratio (KLCR) relative to Carbob ( $\varepsilon = 5.95$ ). .	64
7.4. Performance results of different fuels at BPCR. . . . .	65
7.5. Increase in <i>IMEP</i> relative to Carbob each blend operating at BPCR. . . . .	66
7.6. Differences in spark timing and compression ratio at 600 rpm and 900 rpm. . .	67
7.7. Exhaust gas temperature and adiabatic burnt gas temperature. . . . .	67
7.8. Cumulative net heat release of different fuels. . . . .	68
7.9. Ignition delay and combustion interval of different blending levels . . . . .	69
7.10. Mass fraction burnt for different low level MixedAlcohol blends under equal operating conditions. . . . .	69
7.11. Mass fraction burnt of high level MixedAlcohol blends under equal operating conditions. . . . .	70
7.12. Crank angle degree where 50% of the bulk is burnt (CA50). . . . .	70
7.13. Cycle emissions of different MixedAlcohol blends operating at their BPCR. . .	71
7.14. Increase in THC emission relative to Carbob operating at BPCR. . . . .	72
7.15. Increase in $\text{NO}_x$ emission relative to Carbob operating at BPCR. . . . .	73
7.16. Increase in CO emission relative to Carbob operating at BPCR. . . . .	74
7.17. Increase in brake specific emissions relative to Carbob operating at their BPCR. .	74
7.18. Increase in cycle emissions relative to Carbob operating at their BPCR. . . . .	75



# List of Tables

1.1. Composition of MixedAlcohol. . . . .	3
2.1. Engine operating conditions for determination of research octane number (RON) and motor octane number (MON). . . . .	9
2.2. Chemical and thermophysical properties of alcohols and Carbob. . . . .	12
2.3. Lower heating values of higher alcohols. . . . .	15
4.1. Waukesha CFR F4 engine specification. . . . .	29
4.2. Difference in camshaft design and valve opening time. . . . .	31
5.1. Composition of reference fuels. . . . .	39
5.2. Properties of different MixedAlcohol–Carbob blends. . . . .	40
5.3. Abstract of Standard operating conditions according to ASTM D 2699. . . . .	41
5.4. Operating conditions in the applied DON–procedure. . . . .	43
5.5. Operating conditions for performance tests. . . . .	46
7.1. Determined octane number (DON) of alcohols in comparison with RON. . . . .	61
7.2. Determined octane number of different blends. . . . .	62
7.3. Best combination of compression ratio and spark timing for different blends. . . . .	64
B.1. Physical and chemical properties of alcohols and non-oxygenated gasoline. . . . .	92



# 1. Introduction

This thesis was completed during a stay as a Visiting Research Scholar in the Department of Engineering at the University of California, Berkeley<sup>a</sup>. All the experiments were conducted on a single cylinder research engine at the Combustion Analyses Laboratory<sup>b</sup> which is supervised by Professor Robert W. Dibble.

The increase in efficiency is a driving key for several engineers around the world. The heavy use of fossil fuels has led to a number of serious consequences that we all must face. Above all these effects is global warming which has already had serious environmental and economic impacts. Global warming is caused by an increase in greenhouse gases<sup>c</sup>. Unfortunately, carbon dioxide  $CO_2$ , a greenhouse gas, is one of the by-products of complete combustion. The only possible way to reduce the amount of  $CO_2$  is by either reducing the amount of fossil fuels consumed or by replacing the fossil fuel by a net low carbon equivalent.

The transportation sector accounted for 13.1%<sup>c</sup> of the global anthropogenic greenhouse gas emissions in 2004. Consequential, an increase in efficiency of engines has a profound impact on our environment. Alternative fuels offers new prospects in increasing the efficiency of an engine by simultaneously using a net low carbon fuel. In 2008 a 5.5% fraction in energy content<sup>d</sup> of gasoline and diesel was substituted by biofuels in Austria whereas the objective of the European Union is a 10% fraction by the year 2010. Not just the European Union but also other countries like the U.S. follow this route. In order to utilise all advantages biofuels offer, basic as well as applied research has to be done.

In this thesis the performance and emissions of higher order alcohols is analysed. Ethanol is already widely used as a blending agent for gasoline. It has a higher resistance against knock compared to standard gasoline. Therefore the use of ethanol in an internal combustion engine enables operation at a higher compression ratio. Equation 1.1 shows the connection between

---

<sup>a</sup>University of California, Berkeley: <http://www.berkeley.edu/>

<sup>b</sup>Combustion Analyses Laboratory: <http://www.me.berkeley.edu/cal/>

<sup>c</sup>Intergovernmental Panel of Climate Change, *IPCC Fourth Assessment Report (AR4)*, <http://www.ipcc.ch/> (August 2009).

<sup>d</sup>Bundesministerium für Land- und Forstwirtschaft, Umwelt und Wasserwirtschaft, *Biokraftstoffe im Verkehrssektor 2009*.

the efficiency of an Otto engine and the compression ratio.

$$\eta_{Otto} = 1 - \frac{1}{\varepsilon^{\kappa-1}} \quad (1.1)$$

Where  $\eta_{Otto}$  denotes the efficiency of an ideal air standard Otto cycle,  $\varepsilon$  the compression ratio and  $\kappa$  the ratio of gas specific heat capacities. The strong dependence of the efficiency on the compression ratio leads to a desire of increasing this. Fuels which are more resistant against knock can provide a significant increase in compression ratio.

## 1.1. The Project

The project<sup>e</sup> entitled “An Investigation of a Thermochemical Process for the Conversion of Biomass to Mixed Alcohol” was initiated in 2007 and funded with \$3 million for 3 years. The project is a collaboration between the Universities of California at San Diego, at Davis and at Berkeley and the industrial partner West Biofuel, LLC<sup>f</sup>.

The purpose of this research project is to investigate a thermochemical process for the conversion of biomass to a renewable mixed alcohol fuel. Forest waste, agricultural plant waste, urban green waste and municipal urban waste are possible feedstocks and makes this biofuel a so-called second generation biofuel (cf. Chapter 1.2). This conversion process provides the potential to recycle the large biomass waste stream feedstocks in California by contributing almost no net carbon dioxide ( $CO_2$ ) emission.

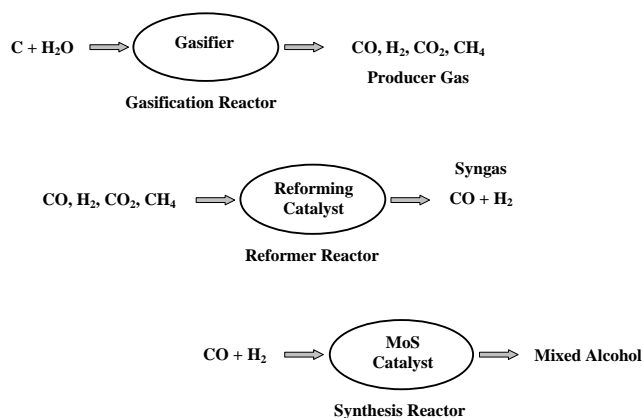


Figure 1.1.: Schematic view of the thermochemical conversion of carbon in biomass to a MixedAlcohol liquid fuel.

<sup>e</sup>University of California, San Diego, Division of Physical Sciences:

<http://physciences.ucsd.edu/molecules/multimedia/images/BiofuelsResearchPlan.pdf>

<sup>f</sup>WestBiofuels, LLC: <http://www.westbiofuels.com/>

Therefore WestBiofuels provides a biomass to mixed alcohol research reactor based on a three-step process (see Figure 1.1). Biomass is firstly gasified to producer gas, secondly reformed to syngas and thirdly synthesised to a liquid mixed alcohol fuel. The mixed alcohol fuel produced by the synthesis of syngas has been granted registration by the US Environmental Protection Agency allowing to be used as a blend agent in gasoline or diesel.

Table 1.1 shows the resulting mixed alcohol composition from the process. Methanol, the simplest of the alcohol molecules, increases the Reid vapour pressure and is therefore limited by regulation to a 3% fraction in gasoline. Consequently the mixed alcohol baseline composition is limited to be no more than 10% in gasoline. A recycling of methanol allows the use of the mixed alcohol with methanol recycle blend (in this thesis termed MixedAlcohol) up to higher blending level. Hence, MixedAlcohol can be used as an E85 blend with no increase in Reid vapor pressure. Part of this research project is the investigation of MixedAlcohol

Alcohols	Mixed Alcohol Baseline Composition	Mixed Alcohol with Methanol Recycle (MixedAlcohol)
Methanol	28%	-
Ethanol	50%	75%
Propanol	16%	11%
Butanol	4%	8%
Pentanol	2%	6%

Table 1.1.: Mixed alcohol composition for MoS based catalyst and composition with methanol recycle.

fuels in internal combustion engines. Octane rating, engine performance determination and emission characterization for eventual fuel qualification of the MixedAlcohol fuel has been done at the Combustion Analysis Laboratory, Berkeley in the standard engine for octane rating, the single cylinder cooperative fuel research engine (CFR).

## 1.2. Biofuels

In the last decade new technologies for the production of biofuels have developed and the biofuel business has grown strongly. A lot of research is done in this field all over the world resulting in new ways of producing biofuels.

So-called first generation biofuels are commercially available and used all over the world, mostly as a blending agent. First generation biofuels are produced by fermentation where sugar, corn or wheat are some of the possible feedstocks. The life-cycle analysis of first generation biofuels is nowadays considered to exceed those of fossil fuels. For example, Searchinger et al. [26] claims that “corn-based ethanol, instead of producing a 20% savings, nearly doubles greenhouse

emissions over 30 years and increases greenhouse gases for 167 years”. These numbers arise due to the consideration of carbon emissions that occur due to a change in land-use. Another downside of food-based biofuels is the competition with food production. For example, the price of sugar reached a 28 year high due to the higher demand of sugar for the production of ethanol<sup>§</sup>. However, both critical examples on biofuels are related to first generation biofuels and ask for a different way of deriving biofuels.

One goal in the production of biofuels is to avoid competition with food production entirely. It is important to mention that not just the feedstock itself may be considered but also the change in land-use. Land used for the production of feedstocks for biofuels could be used instead for growing food. First generation biofuels are limited in production mostly due to their impact on food-supply and biodiversity. As the demand in substitutes for gasoline is increasing, better technologies have been developed enabling a production of so-called second generation biofuels.

Such biofuels are produced from non-food related feedstocks whereas the objective of a higher production output is a key driver. Possible feedstocks for the production of second generation biofuels are biomass, municipal solid waste, agricultural residues etc. where the focus is put on using waste in all different occurrences.

Third generation biofuel is a biofuel from algae. Currently algae fuel is not commercially available but has “been on the horizon but consistently been ‘5 to 10 years’ away from commercial deployment”<sup>h</sup>.

Alternative fuels such as alcohols have the potential to lower greenhouse gas emissions due to a sustainable way of generation. Essential for the creation of a profitable biofuel business, what will be the cornerstone for the success of biofuels, will be the development in fuel prices and the political commitment to renewable energy. So far the production of alcohols is not economically viable and nations choice to push alternative fuels was mostly based on the desire for independence from oil imports. Politics have the power to create a pro-biofuel environment by driving the development and deployment with appropriate changes in energy policy.

### 1.3. Thesis Overview

**Chapter 2** provides an introduction to the basic chemistry of fuels, especially primary reference fuels and alcohols while alcohols are presented in more detail.

**Chapter 3** provides an overview of the basic concepts of combustion with an emphasis on abnormal combustion.

---

<sup>§</sup>BBC, *Sugar price reaches 28-year high*, <http://news.bbc.co.uk/2/hi/business/8193390.stm> (August 2009).

<sup>h</sup>Renewable Fuels Agency, *The Gallagher Review of the indirect effects of biofuels production*, <http://www.renewablefuelsagency.org/> (Mai 2009)

**Chapter 4** provides an explanation and description of the engine itself as well as the engine test bench, including the data acquisition system and the Horiba gas analyser. Further the modifications made on the engine are presented and discussed.

**Chapter 5** presents the experimental procedure established for octane number determination. Further a summary on the standard test method for research octane number determination is given and the differences discussed.

**Chapter 6** provides a summary of different published methods for knock detection and describes the used knock-detection methods. These methods, like integral modulus of pressure oscillations (*IMPO*) or the heat release analysis, are presented in more detail. The indicators used in the performance analysis, like the integrated mean effective pressure (IMEP), are also presented. MATLAB was used as a tool to numerically analyse pressure data.

**Chapter 7** presents the results gained from the experiments. Octane ratings as well as performance analysis and exhaust emissions as well as a discussion of the results.

**Chapter 8** the work presented in this thesis is summarised and future directions of research are shared.





## 2. Fuel Chemistry

Fuel is generally considered as any material, that is burnt or altered in order to transform its energy content into a different form. Nowadays, gasoline derived from petroleum in refineries is the most common fuel used in automotive applications in the U.S. Fuels are mostly a mixture of hydrocarbons with bonds between hydrogen and carbon atoms. These bonds are broken in combustion, new bonds with oxygen atoms are formed and chemical energy is released [27]. The different compounds are categorized according to their number of carbon atoms. Chemical properties are effected by the size and geometry of the molecules as well as the type of bonds (single, double or triple bond).

Not just the molecular formula but also the chemical structure determines the characteristics of a molecule like the boiling point or the latent heat of vaporisation. Further, the structure of a molecule significantly affects the octane rating of a fuel with long, straight chain molecules being more prone to autoignition compared to branched and aromatic hydrocarbons being more resistant. This explains why the octane number of paraffins decreases with carbon number.

Carbob is the non-oxygenated gasoline which was used as the base line fuel for mixing different blends between MixedAlcohol and Carbob. Carbob stands for “California before oxygenated blend” and is a product of Chevron<sup>a</sup>. Unfortunately neither a chemical composition nor specific physical properties of the fuel could be determined. For this reason all chemical properties of Carbob were defined to be the same as the ones published by Gautam et al. [12]. Gautam et al. also used a non-oxygenated gasoline – the so-called UTG96 – which is assumed to be similar but has a slightly higher octane number.

### 2.1. Hydrocarbons

Carbob, the non-oxygenated gasoline used as the base line purely consists out of hydrocarbons. n-Heptane, iso-octane and toluene are hydrocarbons also used in this work as reference fuels. In the following section these hydrocarbons are outlined primarily from a chemical point of view.

---

<sup>a</sup>Chevron Corporation: <http://www.chevron.com/>

## Intermolecular forces

Intermolecular forces are attractions between molecules and in terms of hydrocarbons van der Waals dispersion forces and dipole–dipole forces exist. Van der Waals forces are attractions between atoms or molecules and are of electrical nature. Atoms are in average free of distortions but electrons are mobile and produce dipoles. At any instant one end could be short of electrons, hence making this end slightly positive charged, but at any other instant it could be the opposite. If molecules approach the slightly negative charge side attracts the slightly positive charged side. As electrons move, a constant alternation happens and dipoles change constantly. The strength of dispersion forces depends on the size and shape of an atom. The bigger an atom the higher the number of electrons and also the the radius. More electrons and a higher distance for the electrons to move means a higher possibility for temporary dipoles. Thus, the bigger the atom the higher is the boiling point.

### 2.1.1. Alkanes (Paraffins)

An alkane, the major component in gasoline, is a chemical compound solely existing of carbon and hydrogen atoms with the general formula  $C_nH_{2n+2}$ . The number  $n$  denotes the number of carbon atoms. The atoms are connected in single bonds and therefore called saturated. Normal alkanes, indicated by the prefix  $n$ - for normal, are straight chain alkanes. Isomers are compounds with the same molecular formula but different structural formula [30]. Alkanes with more than 3 carbon atoms can be arranged in a multiple number of ways, hence with fairly different characteristics.

The two components used for PRF in the range 0÷100 are iso–octane and n–heptane. Iso–octane (2,2,4 Trimethylpentane) is an octane isomer and is by definition the 100 point on the octane rating scale. Its general chemical formula is  $C_8H_{18}$ . Actually, the chemically correct name is 2,2,4–Trimethylpentane whilst the numbers 2,2,4 indicate the carbon atom to which the methyl groups ( $CH_3$ ) are attached. n–Heptane is an heptane isomer and is by definition the 0 point on the octane rating scale. Its chemical formula is  $C_7H_{16}$ .

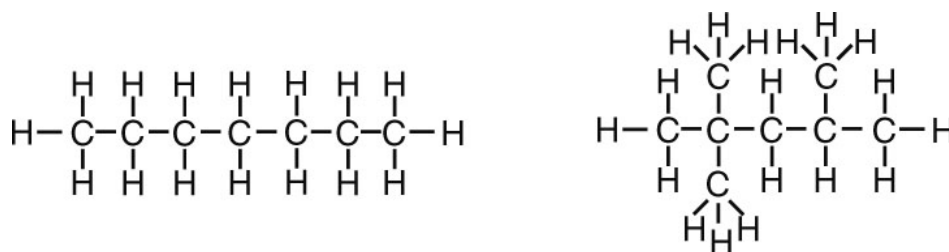


Figure 2.1.: n-Heptane ( $C_7H_{16}$ ) and 2,2,4 Trimethylpentane ( $C_8H_{18}$ ) [11].

## Sensitivity of Fuels

Fuels exhibit different resistance against knock under different operating conditions. The test methods to determine the research octane number (RON) and the motor octane number (MON) differ in significant points. Their main operating conditions are summarised in Table 2.1. The sensitivity of a fuel is a way to show the differing knocking tendencies under

Engine Parameter	Research Method	Motor Method
Engine Speed	600 1/min	900 1/min
Intake Mixture Temperature	52 °C	149 °C
Spark Advance	13° BTDC	19° to 26° BTDC

Table 2.1.: Engine operating conditions for determination of research octane number (RON) and motor octane number (MON).

different conditions and is defined as the difference of RON minus MON. Hence, a sensitive fuel will have a lower MON by definition. Paraffins are considered non-sensitive fuels whereas olefins, aromatics and alcohols are considered to be sensitive. According to Leppard [17] considering olefins and aromatics (sensitive fuels) as the standard and not paraffins (non-sensitive fuels) help in understanding the chemistry of octane sensitivity. From this point of view – considering the autoignition chemistry of olefins and aromatics as ‘normal’ and comparing the autoignition behaviour of paraffins with the ‘normal’ – leads to a super-rated MON [17].

## NTC Behaviour of Paraffins

The term negative temperature coefficient behaviour is derived from low temperature autoignition studies accomplished in static reactors. Thereby fuel and oxidizer are added into a heated reaction vessel and the required time to autoignition is determined as a function of the initial reactor temperature and pressure. According to the Arrhenius law (2.1)

$$\tau = A \cdot e^{\frac{B}{T}} \quad (2.1)$$

where  $\tau$  is the ignition time delay,  $T$  the temperature,  $A$  an preexponential factor and  $B$  a factor proportional to the activation energy, the ignition time delay shows a monotonic decrease as the temperature is increased. Figure 2.2 shows the time to autoignition over temperature for the fuel propane in a static reactor. In the temperature range of 600–650 K the time to autoignition is not in agreement with classical Arrhenius kinetics which predicts a decrease in induction time with increasing temperature (below 600 K and above 650 K). The behaviour where induction time decreases with increasing temperature is termed negative–temperature–coefficient, or *NTC* behaviour [17].

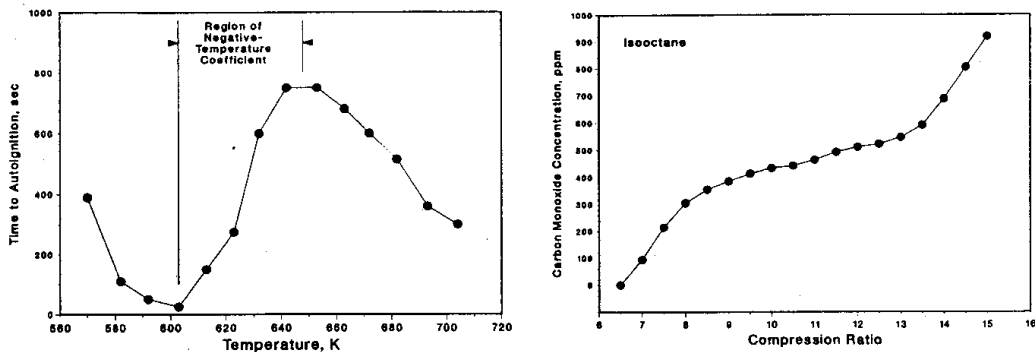


Figure 2.2.: Autignition times for propane as a function of temperature (left) and carbon monoxide concentration of iso-octane as a function of compression ratio (right) [17].

In case of autoignition experiments in an engine the time to autoignition is predefined by engine speed. Temperature and pressure must be varied, e.g. by varying the compression ratio to reach autoignition. Leppard [17] states that carbon monoxide concentration is “a good measure of the extent of autoignition chemistry and a representative stable intermediate species”. Figure 2.2 shows the carbon monoxide concentration as a function of compression ratio for a stoichiometric mixture of iso-octane in air. At compression ratios of 6 to 8.5 and higher than 13.5 the concentration in carbon monoxide increases rapidly and in agreement with the Arrhenius equation. In the compression ratio range of 8.5 to 13.5 the slope in carbon monoxide concentration decreases significantly. This is due to a lower rate of formation of carbon monoxide with increasing compression ratio and is therefore a “manifestation of *NTC* behaviour” [17]. In the motoring experiments Leppard discovered that the *NTC* behaviour was more pronounced at higher temperatures, lower pressures and lower chemical reaction time. Hence, a more pronounced *NTC* behaviour in motor octane rating rather than in research octane rating resulting in a higher compression ratio needed for induced ignition compare to fuels with no *NTC* behaviour (alkenes, aromatics). From this he follows that rather fuels with a *NTC* behaviour have abnormally high motor octane ratings (overrated) instead of calling other fuels sensitive. Pischinger [22] also claims that an adaptation of the octane rating by considering the chemical sensitivity would more realistically present the real resistance of a fuel against knock.

### 2.1.2. Cycloalkanes (Naphthenes)

Naphthenes (Cycloalkanes) are alkanes but the carbon atoms formed in ring structures. As naphthenes bond the atoms only in single bonds they are termed saturated. The general

formula is  $C_nH_{2n}$ .

### 2.1.3. Alkenes (Olefine)

Alkenes, formerly called olefines, have the general Formula  $C_nH_{2n}$  and contain at least one carbon to carbon double bond. Alkenes are termed unsaturated as the double bond can be split and extra hydrogen atoms added. Alkenes have the downside of being prone to oxidation when stored in contact with air. The oxidation products reduce the quality of the fuel and leave gum deposits in the engine [27].

### 2.1.4. Aromatic Hydrocarbon

Methylbenzene (Toluene) ( $C_6H_5CH_3$ ) is based on the benzene molecule  $C_6H_6$  but one hydrogen atom is substituted by a methyl group. Toluene, an aromatic compound, is used as a component for primary reference fuels blends to achieve octane numbers higher than 100.

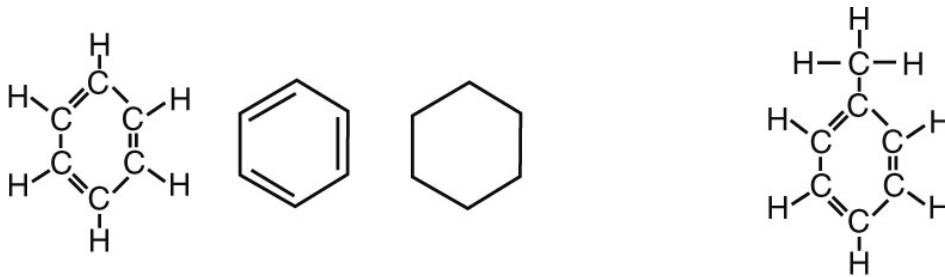


Figure 2.3.: Benzene ( $C_6H_6$ ) and Methylbenzene ( $C_6H_5CH_3$ ) [11].

## 2.2. Oxygenated Hydrocarbons

In terms of oxygenated hydrocarbons only alcohols and ether have significance for the use in internal combustion engines [11]. The term oxygenated hydrocarbons derives from the fact that these hydrocarbons already carry a hydroxyl group (-OH), thus one oxygen atom.

### 2.2.1. Alcohols

Alcohols are compounds in which one or more hydrogen atoms in an alkane have been replaced by a hydroxyl group (OH) [8]. The generic chemical formula is  $C_nH_{2n+1}OH$  whereas methanol ( $CH_3OH$ ) is the simplest possible alcohol. Alcohols can be categorised by the position of the OH-group in the carbon atom chain but also by the number of OH-groups attached. E.g. ethylene glycol ( $C_2H_6O_2$ ), widely used as an automotive antifreeze agent, contains two OH-groups. The three major subsets of alcohols are called primary ( $1^\circ$ ), secondary ( $2^\circ$ ) and

tertiary ( $3^\circ$ ) alcohols based upon how the OH-group is positioned on the chain of carbon atoms [8].

Alcohols offer the essential characteristic being producible out of renewable resources by means of fermentation of sugar, distillation of wood or, as currently explored, out of algae. Their higher resistance against knock makes them an attractive fuel for applications in internal combustion engines.

### Hydrogen Bonding

Intermolecular forces in hydrocarbons were already introduced in Chapter 2.1. Additionally, alcohols have hydrogen bondings as a third intermolecular force beside van der Waals dispersion forces and dipole-dipole attractions.

Any molecule which has a hydrogen atom attached directly to an oxygen or a nitrogen is capable of hydrogen bonding. Hydrogen bonding can occur in both, between molecules and within different parts of the molecule. "Hydrogen bonding is the attractive force between the hydrogen attached to an electronegative atom of one molecule and an electronegative atom of a different molecule". In the case of alcohols oxygen is the electronegative atom whereas hydrogen is the positive atom. Molecules with hydrogen bondings will always have a higher boiling point than similarly sized.

### Chemical Properties of Alcohols

In the following chemical properties of higher alcohols of interest for combustion are shown. The composition of the MixedAlcohol blend has already been shown in Chapter 1 and a table summarising the chemical properties of alcohols is provided in Appendix B.

	Ethanol	1-Propanol	1-Butanol	1-Pentanol	Carbob
Molecular mass	46.1	60.1	74.1	88.2	111.2
Density [ $\text{kg}/\text{m}^3$ ]	789.2	803.2	809.8	813.3	739.2
Oxygen content [% wt.]	34.7%	26.6%	21.6%	18.2%	
Stoichiometric air/fuel ratio	8.9	10.3	11.1	11.7	14.5
Boiling point [K]	351	370	391	411	307–480
Heat of vaporisation [ $\text{kJ}/\text{kg}$ ]	837.86	688.85	584.19	503.68	348.88
Flame speed ( $\lambda=1$ ) [ $\text{cm}/\text{s}$ ]	41				34

Table 2.2.: Chemical and thermophysical properties of alcohols and Carbob [6], [13], [16], [18], [32].

**Molecular Mass** The molecular mass can be calculated from the known chemical composition and their molar masses of the atoms. As the number of atoms increases with higher

order of alcohols the molecular mass increases too.

**Specific Gravity** In general, alcohols have a specific gravity higher than gasoline due to their lower molecular mass. The specific gravity increases in agreement with the molecular mass with increasing order of alcohols.

**Oxygen Content** The oxygen content can easily be calculated from the known chemical composition. As the size of the molecules increases but the number of oxygen atom stays constant the mass percentage of oxygen decreases. With decreasing oxygen content the stoichiometric air/fuel ratio increases whilst the heat of combustion decreases compared to alkanes with the equivalent number of carbon atoms.

**Stoichiometric Air/Fuel Ratio** Alcohols have, as already mentioned, a hydroxyl group which significantly reduces the stoichiometric air/fuel ratio and the lower heating value in comparison to gasoline. On the one hand less air is required but on the other hand more fuel has to be injected for stoichiometric combustion. This requires a higher tank capacity for the same mileage but also asks for high requirements from the injector. A detailed calculation of the stoichiometric air/fuel ratio is outlined in Appendix 3.1.

**Boiling Point** The boiling point of alcohols increases with the number of atoms, hence the size of the molecule. The hydrogen bonding and the dipole–dipole interactions are almost the same for all alcohols but the van der Waals dispersion forces increase with the size of the alcohol. However, more energy is required to overcome the dispersion forces which in turn leads to an increase in boiling temperature. The boiling point of a certain alcohol is always higher than of the equivalent alkane (cf. Figure 2.4). Reason therefore lies in the fact of different intermolecular forces. Van der Waals attraction exists in both, alkanes and alcohols, but are much smaller compared to the hydrogen bond which just exist in alcohols. But even by neglecting the hydrogen bonds alcohols would still have a higher boiling point as they have more electrons (oxygen has an extra 8 electrons) which in turn increase the dispersion forces, hence increase the boiling point [8]. But the boiling point of alcohols also increases with the number of carbon atoms because of the intermolecular van der Waals dispersion forces. These forces increase with the length of a molecule whilst the hydrogen bonding and the dipole–dipole forces stay much the same [8].

**Latent Heat of Vaporisation** Latent heat is the amount of energy required during a phase transition. Hence, latent heat of vaporization is the energy required to transform a liquid into a gas. However, vaporisation is an endothermic process as the liquid absorbs energy which is required to break all intermolecular forces. As mentioned above alcohol's hydrogen bonds require rather more energy to break than dispersion forces. Hence,

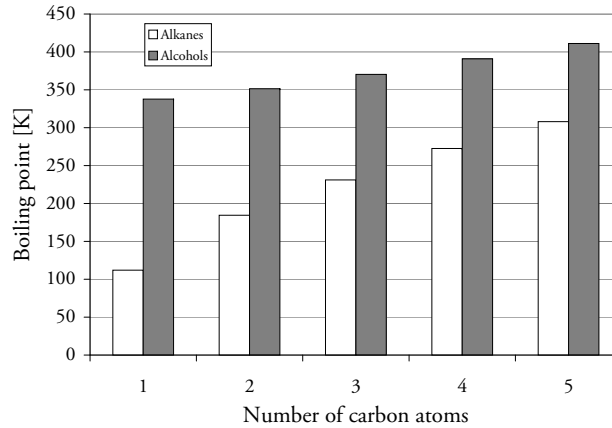


Figure 2.4.: Comparison in boiling points of alkanes and boiling points of alcohols.

alcohol's latent heat of vaporization is significantly higher than equivalent alkane's. As smaller molecules have a higher total number in intermolecular bonds per volume the latent heat of vaporisation decreases with higher alcohols. The energy demand has a positive effect on the octane quality as it cools the intake air down. Further the cooler intake air enables more mass in the cylinder, hence a higher volumetric efficiency. The downside is the hassle in cold start conditions where the high latent heat of vaporisation can lower the charge temperature below the ignition temperature.

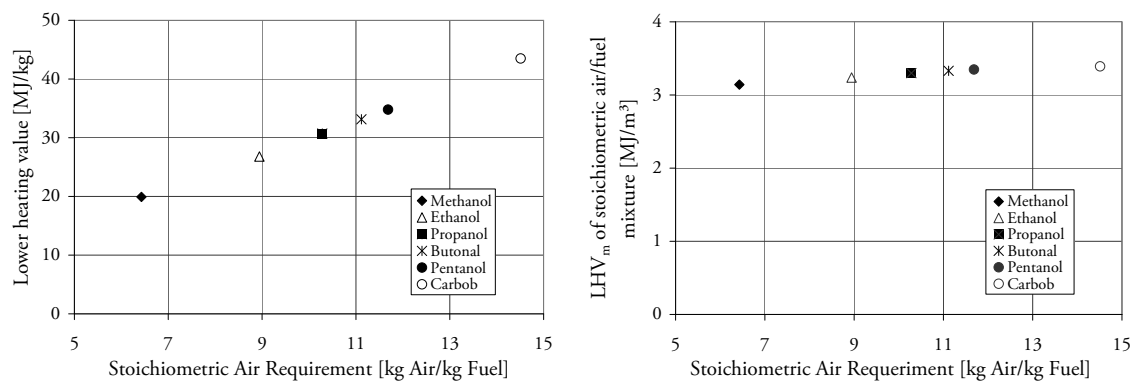
**Flame Speed** In internal combustion engines high flame speeds are appreciated as the constant volume combustion can closely be achieved. Numbers for lower alcohols were found and are higher compared to gasoline. The flame speed of a specific fuel is a function of the air/fuel ratio, the temperature and the pressure. In general, the flame speed increases with higher temperatures while the variation with the air/fuel ratio roughly follows that of flame temperature. In contrast declines the flame speed with increasing pressure.

**Lower Heating Value** Alcohols have a significantly lower heating value than gasoline. Carbon atoms have the highest energy density of all atoms in fuels and as alcohols contain less carbon atoms than gasoline, the lower heating value of alcohols is significantly lower. Although alcohols have a significantly lower heating value than gasoline the heating value of the air/fuel mixture ( $LHV_m$ ) is much closer to gasoline's. Figure 2.5 shows the increasing lower heating value (LHV) with increasing number of carbon atoms, with gasoline the highest. However, the lower heating value of the mixture ( $LHV_m$ ) (cf. Figure 2.5) does not vary as much as the lower heating value LHV of different fuels do (cf. Figure 2.5). Reason therefore is the different stoichiometric air requirement of the different fuels.



	Ethanol	1-Propanol	1-Butanol	1-Pentanol	Carbob
LHV [kJ/kg]	26803	30709	33142	34791	43500
% of Carbob	62%	71%	76%	80%	
LHV [kJ/l]	21148	24659	26679	28320	32320
% of Carbob	65%	76%	83%	88%	
LHV <sub>m</sub> [kJ/m <sup>3</sup> ]	3239	3299	3330	3349	3392
% of Carbob	95%	97%	98%	99%	

Table 2.3.: Lower heating values of higher alcohols.

Figure 2.5.: Lower heating value (LHV) of different fuels (left) and lower heating value of stoichiometric air/fuel mixtures (LHV<sub>m</sub>) at:  $\lambda=1$ ,  $p=1$  bar,  $T=300$  K (right).

### 2.2.2. Ether

Ether is an organic compound that contains an oxygen atom connected to two alkyl groups and it is often used as a solvent. In some countries health complaints like headaches, nausea, dizziness and breathing difficulties were reported after gasoline containing MTBE was introduced [25]. However, data available on human exposure data to MTBE are limited but experiments with rats showed that at relatively high levels of MTBE reversible neurobehavioural changes were observed [25].

## 2.3. Additives

All gasoline nowadays available at petrol stations is enriched with additives. Increasing the octane number of fuels is one of the main purposes of an additive. Therefore, so-called antiknock agents like toluene, ethers or alcohols are added. But also corrosion inhibitors, anti-oxidants (prohibit gum formation), anti-icing, different lubricants and also deposit-modifying additives to lower deposits in fuel injectors or intake valve play an important role in order to lower the

failure rate of parts. The ratio of additives in fuels is regulated.

## 3. Combustion

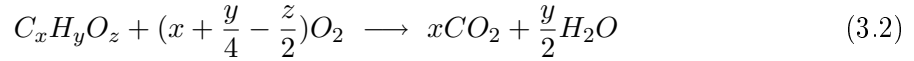
In this chapter the fundamentals of combustion in internal combustion engines are outlined whereas the differences between normal combustion and abnormal combustion are presented in more detail. Further the mechanism in the formation of nitrogen oxides and hydrocarbons are described.

### 3.1. Stoichiometric Air Requirement

The stoichiometric air requirement is defined as

$$Air_{st} = \frac{m_{Air,st}}{m_{Fuel}} = \frac{m_{O_2,st}}{m_{Fuel}\xi_{O_2,Air}} . \quad (3.1)$$

with the index *st* referring to stoichiometry. In combustion of a hydrocarbon fuel the stoichiometric air requirement is defined by the oxygen required in the chemical reaction



whereas the required oxygen is illustrated by the term

$$n_{O_2,st} = (x + \frac{y}{4} - \frac{z}{2})O_2 \frac{kmol O_2}{kmol Fuel} . \quad (3.3)$$

It comprises of the oxygen required for stoichiometric combustion by the carbon and hydrogen atoms reduced by the oxygen atoms already provided by the molecule. The composition of air can be approximated by 79% nitrogen and 21% oxygen whereas the mass fraction of O<sub>2</sub> in air is given by

$$\xi_{O_2,Air} = \frac{m_{O_2,Air}}{m_{Air}} = \frac{n_{O_2,Air}}{n_{Air}} \frac{M_{O_2}}{M_{Air}} . \quad (3.4)$$

By combining equation 3.1 and 3.3 and 3.4 the stoichiometric air requirement can be calculated as

$$Air_{st} = \frac{1}{\xi_{O_2,Air}} \frac{n_{O_2,st}}{n_{Fuel}} \frac{M_{O_2,st}}{M_{Fuel}} . \quad (3.5)$$

For a more detailed derivation of this equation see Appendix A.

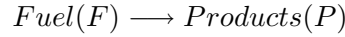
## 3.2. Normal Combustion

Normal combustion in a spark ignition engine is when the air/fuel mixture in close proximity of the spark plug is ignited by a spark and due to the propagation of the flame the rest of the air/fuel mixture burns without any pre-ignition or detonation.

### 3.2.1. Thermal Ignition – Ignition Process

The ignition process is the initial event to make combustion happen. In spark ignition engines the air/fuel mixture is ignited by a spark plug whereas in compression ignition engines the air/fuel mixture autoignites once a certain pressure and temperature is reached.

Ignition is a time-dependent process starting with reactants and evolving in time towards a steadily burning flame [29]. Semenov (1935) established an ignition-model based on a spatially homogeneous system, i.e. pressure, temperature and composition are uniform, and the chemistry is approximated the following one-step reaction



with the first order reaction

$$r = -M_F c_F A * \exp(-E/RT) \quad (3.6)$$

with the molar mass  $M_F$  of the fuel, a fuel concentration of  $c_F$ , a pre-exponential factor  $A$  and an activation energy  $E$ . The fuel consumption during the ignition process is small and by neglecting reactant consumption the reaction rate can be simplified to [29]

$$r = -\rho A * \exp(-E/RT). \quad (3.7)$$

Heat transfer, hence the loss term, is modelled with Newton's law of heat exchange. The heat flux  $j$  is equal to

$$j = \chi S(T - T_W) \quad (3.8)$$

where  $T$  denotes the temperature in the system,  $T_W$  the temperature of the walls,  $S$  the heat transfer surface and  $\chi$  the heat transfer coefficient. The heat transfer coefficient is dependent on the temperature and the geometry of the system, hence approximations have to be made. The temperature of the system is time-dependent and can be calculated from an imbalance of heat production  $P$  and heat transfer  $L$  (loss) of the system.

$$\rho c_P \frac{\partial T}{\partial t} = P - L = (h_F - h_P) \rho A * \exp(-E/RT) \chi S(T - T_W) \quad (3.9)$$

The term  $h_F - h_P$  denotes to differences in the enthalpy of the fuel products, hence the heat released by the reaction.

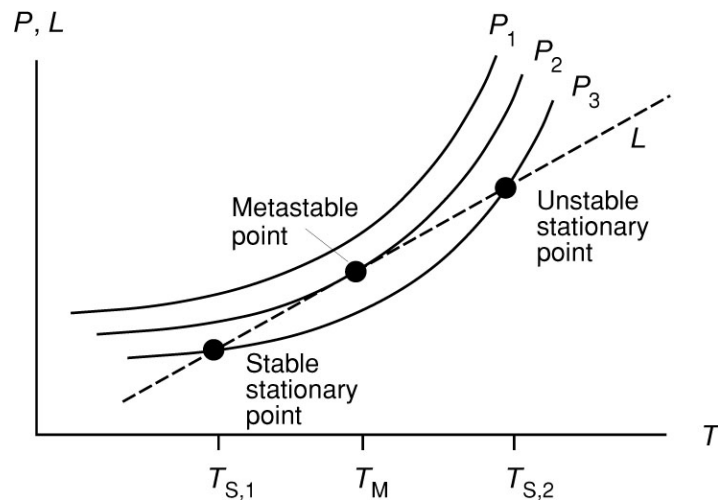


Figure 3.1.: Schematic illustration of the temperature dependences of heat production ( $P$ , solid line) and heat losses ( $L$ , dotted line) [29].

By plotting the production term as well as the loss term in a graph the qualitative behaviour of the system can be understood (see Fig. 3.1). The linear increase of the loss term with increasing temperature can already be seen in equation 3.8 whereas the exponential increase of heat production with rising temperature can be seen in equation 3.7. Figure 3.1 shows three different heat production terms whereas each has a different product of activation energy  $E$  and preexponential factor  $A$ . Intersections between the heat loss term  $L$  and the production term  $P$  mark points of equal heat productions and heat losses and are called stationary points. Considering curve  $P_3$  and a temperature  $T < T_{S,1}$  heat production dominates and the temperature of the system increases until heat production and heat losses are equal, thus until  $T_{S,1}$  is reached. If the temperature is  $T_{S,1} < T < T_{S,2}$  heat losses dominate and the system cools down until heat production and heat loss equal, thus until  $T_{S,1}$  is reached. Therefore point  $T_{S,1}$  is called a stable stationary point. At temperatures  $T > T_{S,2}$  the system is dominated by heat production, the temperature keeps increasing and causes the reaction to further accelerate what leads to an explosion. The point  $T_{S,2}$  is a so-called unstable stationary point because any small deviation leads either to an explosion or a cooling down of the system to the stable stationary point  $T_{S,1}$ . If the temperature of the system is equal to  $T_M$  any infinitesimal increase in temperature leads to an explosion and any infinitesimal decrease in temperature leads to a cooling down to point  $T_{S,1}$ . If the production term is equal to curve  $P_1$  the system will explode for all initial temperatures as the production term exceeds the loss term in any point.

### 3.2.2. Autoignition – Ignition Limits

Ignition limits, hence limits as to which temperature, pressure and composition a certain mixture can be ignited, is essential in combustion. Ignition delay times are determined by taking the time a mixture in a vessel under certain values of temperature and pressure needs to ignite, ranging from as long as hours to as short as microseconds. If no ignition occurs just a slow reaction happens. Figure 3.2 shows a  $p$ - $T$  explosion diagram in which the regions of explosion or slow reaction (no ignition) are separated by a curve.

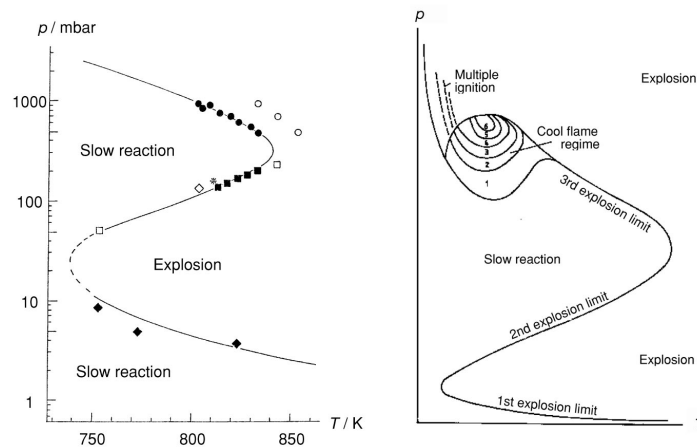


Figure 3.2.: Ignition limits ( $p$ - $T$  explosion diagram) for hydrocarbons [29].

Considering a temperature of 800 K and a pressure below 5 mbar the mixture does not ignite in the curve in the left picture but a slow reaction occurs. Reason therefore is that reactive radicals which are formed in the gas phase diffuse to the vessel wall where they recombine to stable species. The diffusivity is inversely proportional to the density, hence diffusion is fast at low pressures. By increasing the pressure the diffusion rate decreases ( $D \propto p^{-1}$ ). However, at a certain pressure the production of radicals exceeds the diffusion of the radicals with lower diffusion coefficients to the wall where radicals recombine to a stable species. Above the first explosion limit the mixture spontaneously ignites. This limit strongly depends on the chemical structure of the walls as the limit is a result of the “concurrent processes of chain branching in the gas phase and chain termination at the surface” [29]. Above the second explosion limit chain termination in the gas phase always exceeds chain branching in the gas phase, hence no ignition but just a slow reaction happens. The second explosion limit is driven by the concurrent processes of chain branching and chain termination in the gas phase whereas chain termination always exceeds chain branching. The third explosion limit is the thermal explosion limit as described in chapter 3.2.1 which is determined by the difference in heat production by the chemical reaction and heat losses to the wall.

Explosion limits, especially the third one, are more complex, mostly due to additional chem-

ical reactions (e.g. formation of hydroxydes) [29]. At low temperatures and high pressures, regions can be found where ignition takes place after the emission of short light pulses (multi-stage ignition) or regions where combustion takes place at low temperatures (cool flames).

### 3.2.3. Autoignition – Ignition Delay Time

Typical for purely thermal explosion (described in chapter 3.2.1) is the sudden rise in temperature. In hydrocarbon/air mixtures it can be observed that an explosion happens after a certain ignition delay time. During the ignition delay time, radical–pool population is not high enough to consume enough fuel for an explosion. However, important chemical reactions take place, e.g. chain branching, formation of radicals, whilst the temperature stays almost constant. But with increasing populations in radicals the consumed fuel fraction increases and rapid ignition happens.

There are several different models describing the dependence of the ignition delay time on pressure and temperature. A widely accepted model is in agreement with and based on the Arrhenius law [23]

$$\tau = Ap^{-n}e^{\frac{B}{T}} \quad (3.10)$$

where  $\tau$  denotes the ignition delay time,  $A$  a preexponential factor,  $p$  the pressure,  $n$  an exponent considering the pressure,  $T$  the temperature and  $B$  a factor proportional to the activation energy. The constants  $A$ ,  $B$  and  $n$  are derived from experiments and dependent on the type of fuel.

### 3.2.4. Detonation

“Usually, flame propagation (deflagration) happens due to chemical reaction that sustains a gradient in temperature, pressure and species concentration and the molecular transport processes that propagate the gradient. In contrast, detonations propagate due to a pressure wave sustained by a chemical reaction and the corresponding heat released” [29]. Characteristically, detonations propagate with flame speeds higher than 1000 m/s what is based on the high speed of sound in the burnt gases. Detonations in respect to internal combustion engines is outlined in Section 3.3.2.

## 3.3. Abnormal Combustion

Knocking is the limit in spark ignition engines and is arguably as old as the IC engine itself. In personal records of Nicolaus August Otto dated from the year 1862 during experiments he conducted in his first 4 stroke research engine he note “... 1862 lief dieselbe und war auch in demselben Jahr total ruiniert durch die heftigen Stöße, welche in derselben auftraten.”[22]

### 3.3.1. Surface Ignition

Surface ignition is caused by the mixture igniting as a result of contact with a hot surface such as hot exhaust valves, incandescent combustion deposits or a hot spark plug (wrong heat rating of the spark plug). Surface ignition happens independently from the actual spark ignition and often leads to a so-called run-on or dieseling; what means the engine continues to fire after the ignition has been switched off.

#### Pre-Ignition

Pre-ignition is surface ignition in advance of the spark and leads to a higher in-cylinder pressure. A higher pressure increases the compression work what in turn causes a reduction in power. Further the peak pressure boosts self-ignition, thus a higher compression ratio enhances self ignition.

It has to be mentioned that pre-ignition and knocking combustion are separate events although their effect can be similar. Both events increase the combustion temperature significantly, hence, either event increases the probability of the other event to commence. Both can lead to rough engine operation, mechanical damage and also engine failure. Menrad [20] conducted pre-ignition experiments with an electrically heated coil used as a ignition source whereas the power input required to set off pre-ignition was recorded. Menrad concluded that “no relation between pre-ignition rating and octane numbers” [20] could be found but “that pre-ignition would sometimes follow after sustained strong knock” [20].

### 3.3.2. Engine Knock

Knock is still called a phenomena and not fully understood. A pragmatic definition of knock is that it occurs if the octane requirement of the engine exceeds the octane quality of the fuel [17]. However, knocking occurs after the air/fuel mixture was correctly ignited by the spark plug. The flame front propagates away from the sparking plug whilst the unburnt gas is heated up by radiation. Self ignition then happens, if the temperature and pressure in the cylinder reach a certain state that causes the end gas to ignite spontaneously. Thus the pressure rises rapidly, which can be characterised by knocking. Knocking is audible, caused by the resonances of the combustion chamber walls.

In a knocking combustion cycle the in-cylinder pressure transducer records pressure curves with typical high frequency and sometimes high amplitudes as shown in Figure 6.1. This high frequency waves are a superimposition of (main) normal pressure waves and the end gas pressure waves. Shock waves effect a typical pinging noise which varies with the intensity of knock from light metallic pinging sound to a rough ‘hammering’ sound. The high-frequency pressure waves can cause severe erosive damage and high thermal loads on certain engine parts



what can lead to mechanical damage and also engine failure. The significantly increasing heat transfer coefficient with rising temperature greatly increases the likelihood of piston seizure. The rising heat transfer coefficient also raises the likelihood of pre-ignition. If the pre-ignition occurs earlier in the compression stroke the spontaneous ignition will also occur earlier, leading to more severe knock but also to a situation known as run-away knock. The engine will continue to operate although the ignition is turned off.

A lot of different theories about engine knocking have been published so far. Most of them agree that self-ignition is the effect that causes knocking combustion, but different reasons leading to self ignition have been published. However, in the following two general theories on knocking, the compression theory and the detonation theory, as well as theories combining both is outlined.

**Compression Theory** The increase in pressure derives from the piston motion and additionally from the expansion of the burnt gases. This leads to conditions where the end-gas self ignites whereas areas with a low initiation energy are prone to self ignition. Once the mixture ignited at a secondary ignition point the pressure waves cause more ignition points and the end-gas starts to burn rapidly.

**Detonation Theory** Due to a steepening-process of the normal pressure wave it can evolve to a shock wave. In the front of the shock wave self ignition conditions cause the end-gas to self ignite.

**A Combination of Compression and Detonation Theory** This theory combines both theories explained above. It considers self-ignition in the end-gas to trigger a rapid flame development in the end-gas zone which evolves with increasing knock intensity to a shock wave or detonation wave.

The better part of theories about knocking consider self-ignition in the end gas zone as the major reason for knock. Withthrow and Rassweiler<sup>a</sup> have already published this theory in 1936, derived from pictures taken with a highspeed-camera. Curry's<sup>a</sup> theory conceives from an acceleration of the flame propagation. The reason therefore is the formation of radicals in the unburnt gas which in turn constantly raises the speed of flame propagation to the speed of knocking combustion. Curry equipped a research engine with 49 ion current sensors and sweped data from operation conditions where knocking as well as non-knocking cycles occurred. He showed that the burn rate of knocking cycles is already higher before the initiation of knock than in a non knocking cycle and the difference in burn rates is also higher than cycle to cycle variations. He concluded that radicals must already exist before knock is initiated. Curry found a maximum speed of flames of 366 m/s, hence subsonic speed, and derived from this, that knocking is not necessarily connected to detonation.

---

<sup>a</sup>Found in Pischinger [22]

## Operating Conditions Influencing Engine Knock

Combustion in internal combustion engines can be quite sensitive to any change in operating conditions: here the most important ones are briefly summarised. An advance in spark timing promotes a higher peak pressure and therefore higher temperatures, hence the affinity for knock increases with the spark advance. A similar effect has an increase in compression ratio or intake pressure. Both increase the peak pressure what leads to a higher tendency for knock. The volumetric efficiency affects the indicated mean effective pressure proportional. An increase in volumetric efficiency means an increase in peak pressure and therefore higher temperatures, hence an increasing affinity for knock with increasing volumetric efficiency. A higher engine speed leads to higher turbulences in the cylinder. Higher turbulences leave less time for reactions prior to combustion, hence a decrease in knock tendency with increasing engine speed. The octane number of a fuel displays its resistance against knock and differs significantly between different fuels. In terms of the air/fuel ratio more factors have to be considered. An increase in the air/fuel ratio increases the charge temperature in the cylinder due to a lower cooling effect resulting in a higher burned gas temperature which in turn increases the heat transfer. Contrary the laminar flame speed decreases in lean combustion. However, studies showed a distinct affinity for knock at an air/fuel ratio of 0.95 [22]. Lowering the intake temperature results on the one hand in a lower process temperature and on the other hand in a higher volumetric efficiency. The lower temperature overcompensates the higher volumetric efficiency resulting in a reduction of knock affinity with lower temperatures. Several studies proof that an asymmetrical location of the spark plug, like in the CFR, enhances knocking combustion [22] [28]. However, a centrally located spark plug as well as quenching zones which focus the air/fuel mixture around the spark plug lower the affinity for knock.

## 3.4. Formation of Pollutants

The formation of emissions (*CO*, *NO<sub>x</sub>* and *HC*) in an internal combustion engine depends on operating parameters like ignition timing, load, speed and especially the air/fuel ratio. Carbon monoxide is formed due to incomplete combustion which occurs in fuel-rich mixtures. In fuel-lean mixtures carbon monoxide is formed due to dissociation. The mechanism in the formation of nitrogen oxides and hydrocarbons are outlined in the following chapters.

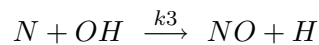
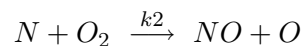
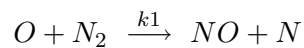
### 3.4.1. Nitrogen Oxide Formation

“The mixture of nitric oxide (*NO*) and nitric dioxide (*NO<sub>2</sub>*) is referred to as *NO<sub>x</sub>*” [27]. *NO<sub>x</sub>*, although being a less obvious product of combustion, is a major contributor of photochemical smog and ozone. Nitric oxide is usually by far the dominant formed nitrogen oxide during

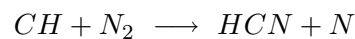
combustion. Nonetheless, nitric dioxide is formed by further oxidation in the environment and is the much more hazard pollutant on the environment.

Four different routes in the of formation  $NO_x$  are identified [29]: the thermal route, the prompt route, the  $N_2O$  route and the fuel–bond nitrogen route.

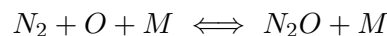
**Thermal NO** or also called Zeldovich  $NO$  is based on the extended Zeldovich mechanism shown below.  $N_2$  molecules have very strong triple bonds, hence a very high activation energy is required. The first reaction with the rate constant  $k1$  is thus sufficiently fast only at high temperatures [29] what is the fundamental explanation why thermal  $NO$  is assumed to occur in the hot combustion gases.



**Prompt NO** results from the radical  $CH$  which is formed as an intermediate at the flame front only.  $CH$  reacts with  $N_2$  of the air to form hydrocyanic acid ( $HCN$ ) which later reacts to  $NO$ . The prompt mechanism comes into play both, when there is fuel–bound nitrogen and also at low temperature combustion when the thermal mechanism is negligible.



**The nitrous oxide ( $N_2O$ ) mechanism** is important in the formation of  $NO_x$  at low temperature combustion. This mechanism is similar to the thermal mechanism but with the presence of a third molecule  $M$ , the outcome of this reaction is  $N_2O$ . Under lean conditions the formation of  $CH$  is suppressed whereas low temperatures can suppress thermal  $NO$ . Remaining is just the  $NO$  formed via  $NO_2$  which is enhanced at high pressures because of the three–body reaction. Three–body reactions typically have a low activation energy what leads to a lower required temperature for the formation through the  $N_2O$  route.



**Conversion of Fuel Nitrogen into NO** has mainly been observed in coal combustion [29] and can normally be neglected in spark ignition engines [27]. However, coal contains about 1% by mass chemically bound nitrogen which evaporates during the gasification process and leads to  $NO$  formation in the gas phase.

### 3.4.2. Hydrocarbon and Soot Formation

Unburnt hydrocarbons are a consequence of local flame extinction [29], either flame extinction by strain or flame extinction in gaps or at walls. Local flame extinction due to strain is often caused by intense turbulence. If the extinct flame does not reignite unburnt hydrocarbons are formed. Rich or lean mixtures are prone to flame extinction as the temperature is lower, hence reaction times may become larger than mixing times [29].

Flame extinction at walls and in gaps are a combination of heat transfer effects as well as removal of reactive intermediates. When a flame approaches a wall which is usually colder than the flame, heat is removed from the flame, hence a cooling of the reaction zone happens. Thereby, a classification in extinction of the flame front parallel to the wall and perpendicular to the wall is made.

**Extinction of a flame front parallel to the wall** Flame fronts need to keep a certain distance to the wall to avoid being quenched whereas the quenching distance is a function of the flame thickness. However, the formation of unburnt hydrocarbons was assumed to result from flame extinction at walls. Further it was assumed that the unburnt hydrocarbons stay in the extinction zone. In the last years, this assumption was first challenged by numerical simulations and later proofed by experiments. Unburnt hydrocarbons do not stay in the extinction zone but rather diffuse into the extinguishing flame. Most hydrocarbons are consumed but still leaving a few [29].

**Extinction of a flame front perpendicular to the wall** The more likely occurrence of a flame front perpendicular to the wall occurs with a higher flame speed than flames parallel to the wall. The higher flame speed leaves less time for hydrocarbons to diffuse into the reaction zone. Hence, more unburned hydrocarbons result from the flame front perpendicular to the wall.

**Extinction of a flame front in a gap** Crevices like the fire land in an engine are major regions for an extinction of the flame.

## 4. Experimental Setup

All experiments were conducted at the Combustion Analyses Laboratory at UC Berkeley. The engine used for all of the results presented in this thesis is a single cylinder research engine, the so-called Cooperative Fuel Research Engine (CFR), model F4. Figure 4.1 displays the setup of the test bench including the CFR engine itself with in-cylinder pressure indication, a standard data acquisition system as well as a Horiba gas analyser to measure emissions concentration in the exhaust. The fuel system contains three pressurised vessels (cf. Chapter 4.1.1) which feed the Bosch fuel injector. The injector is installed in the intake manifold housing downstream the throttle plate and a wideband oxygen sensor measures the proportion of oxygen in the exhaust gas. A Motec M4 engine management system (ECU) enables closed loop control to achieve stoichiometric combustion. Intake as well as exhaust temperature are typically measured by means of thermocouples. Further the test bench is equipped with a Harnischfeger HDM 365 dynamometer to measure torque and a Horiba gas analyser to sample emission data. Not displayed in this schematic view is the coolant system which is presented in detail in Chapter 4.1.2.

The CFR engine is the worldwide standard engine used for testing fuels and lubricants for the internal combustion engine. It is defined in the ASTM D2699 and the ASTM D2700 (DIN EN ISO 5164/DIN EN ISO 5163 respectively) standard for Research Octane Number (RON) and Motor Octane Number (MON) rating respectively as the engine to use. The main reason for being used as a fuel research engine is based on the variable compression ratio of the engine.

Waukesha, the manufacturer of CFR engines, offers a CFR<sup>®</sup> F1/F2 model which fulfils the requirements for RON/MON testing but also a CFR<sup>®</sup> F4 model which is defined as the engine to use in the ASTM D909, the Standard Test Method for Supercharge Rating of Spark-Ignition Aviation Gasoline. At the Combustion Analyses Laboratory a CFR<sup>®</sup> F4 model was provided and used for all conducted experiments. The differences between the F1/F2 and the F4 model are significant and described in Chapter 4.1.1.

### 4.1. Cooperative Fuel Research Engine (CFR)

The CFR engine is a four-stroke, two-valve, single cylinder, spark ignition engine with a variable compression ratio. The engine has a bore of 82.65 mm and a stroke of 114.3 mm, giving a swept volume of 613.23 cm<sup>3</sup>. It is a two-valve engine with an open valve train and a

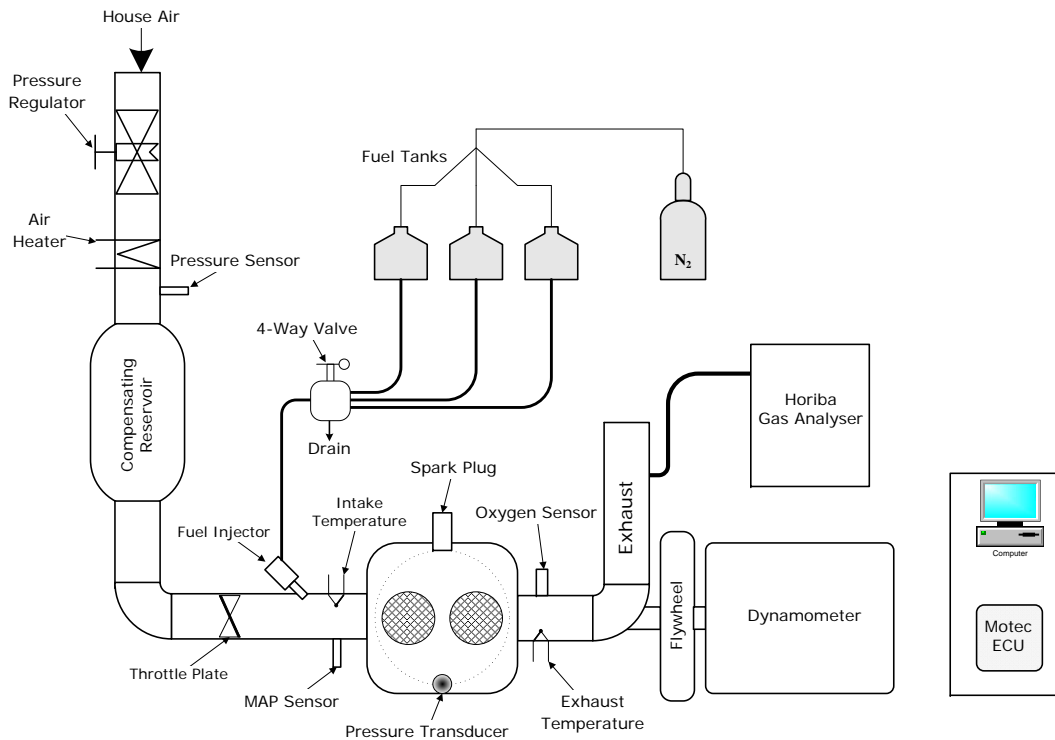


Figure 4.1.: Schematic view of the CFR test bench at the Combustion Analyses Laboratory, at UC Berkeley.

stroke/bore ratio of  $S/B = 1.38$ , hence a long stroke engine. The engine dates from September 1950 and was given as a donation to UC Berkeley. CFR's main characteristics are listed in Table 4.1.

Figure 4.2 provides a cross-sectional view of the CFR engine. As already mentioned, it is a two-valve engine whereas the valves are controlled by an underhead camshaft and push rods. The spark plug is mounted horizontally in the circumference of the cylinder, hence a non-central location. Originally, a detonation meter was installed to detect knocking combustion. Instead, a pressure transducer for pressure indication was mounted with an adapter in the bore actually designed for the detonation meter. The aluminum piston has a flat top and no quench zone, 4 compression rings and one oil ring. The cast iron cylinder head is adjustable at will. A hand crank, which engages through a worm and screw, raises or lowers the cylinder head. By the means of a micrometer the compression ratio for any setting between between 4:1 and 17:1 can be precisely measured. For a change in compression ratio the engine needs not to be stopped and no adjustments on the valves have to be made. By gripping the clamping sleeve the cylinder head gets fixed in position. The inlet and exhaust connections are designed flexible as well as the fuel lines. In the topview the intake valve shroud of the F1 model is

Manufacturer	Waukesha Motor Company - built in 1950
Type	Cylinder jacket water cooled Four stroke cycle engine
Bore	82.65 mm (3.250 in)
Stroke	114.3 mm (4.500 in)
Compression Ratio	Adjustable 4:1 to 17:1
Piston Rings Material	Cylinder: Cast iron Piston: Aluminum
Fuel System	Intake-manifold fuel injection
Ignition	Spark ignited
Camshaft, deg overlap	30
I/O/IVC	15° BTDC / 50° ABDC
EVO/EVC	50° BBDC / 15° ATDC

Table 4.1.: Waukesha CFR<sup>®</sup> F4 engine specification.

displayed. This is one of the significant differences to the F4 model which does not have a shroud on the intake valve (cf. Chapter 4.1.1).

The design of the CFR is determined by its historical development. The first CFR engine for octane rating was produced in the early 1930's and has, beside some crankcase upgrades, hardly changed since then<sup>a</sup>. The main reason therefore is that ratings made in the earliest engines match with ratings done nowadays.

#### 4.1.1. Differences between the CFR F1/F2 model and the CFR F4 model

Any change in setup is crucial to the results and precision is highly important for an accurate octane number determination. Major differences between the two models are in the equipment responsible for mixture preparation. The most important differences affecting the test results are summarised:

- Intake manifold fuel injection instead of a carburetor
- Camshaft design – 5° CA and 30° CA camshaft overlap in CFR F1/F2 and F4 model respectively
- Valve opening – resulting from different camshaft designs, the valve opening time varies significantly between the F1/F2 and the F4 model

<sup>a</sup>WAUKESHA ENGINE DIVISION DRESSER INDUSTRIES INC. *The Waukesha CFR Fuel Research Engine*, 1980.

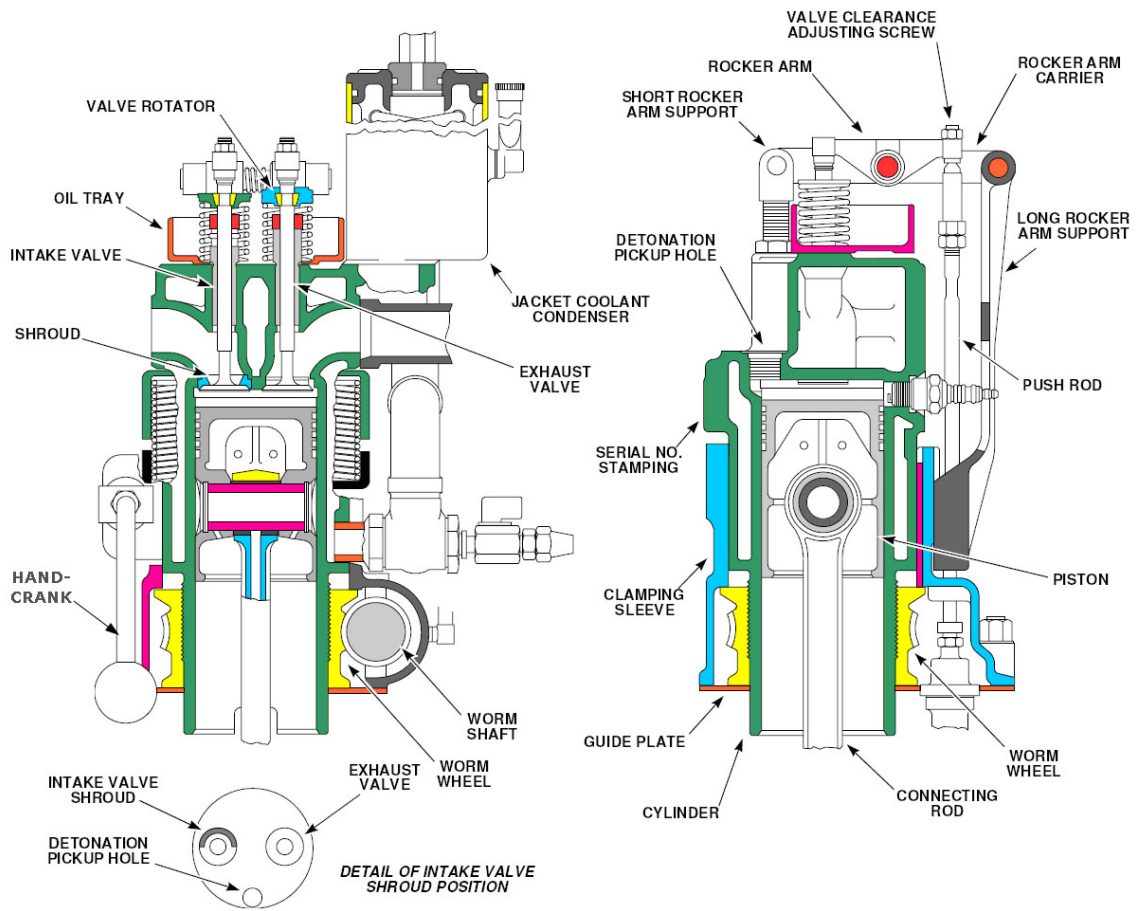


Figure 4.2.: Cross-sectional view of a CFR F1/F2 model<sup>b</sup>.

<sup>b</sup>Dresser Waukesha, *Form 847 "F1/F2 Operations and Maintenance"*, Fig 305-2, 2008.



- Valve design – the F1/F2 model has a shroud on the intake valve whereas the F4 model has a plane intake valve.

### Fuel Delivery System

The standard model for octane rating, the F1/F2 model, is equipped with a carburetor, whereas in comparison the F4 model has an intake manifold fuel injection. The used CFR engine is equipped with a throttle housing originally used on a BMW R1100R motorcycle. The fuel is squirted into the intake manifold by a Bosch injection valve installed in the throttle housing with a pressure of 40 psi (2.76 bar). As with alcohols a higher mass of fuel has to be delivered in some of the experiments the injector reached its limit in providing the required mass of fuel.

In order to keep the fuel as neat as possible a system with little contamination is essential. A new system had to be designed as in the old custom-made system the wastage in fuel and contamination was too high. Pressurised tanks with no fuel return line seemed to be the best option in which nitrogen, a non-flammable gas, is used as the pressurising medium (see Figure 4.2). Three tanks were installed enabling to have three different fuels available simultaneously. The four-way valve before the injector enables to chose between the tanks and makes purging of the fuel pipes between the tanks and the four-way valve with nitrogen possible. Further the four-way valve allows a switch between fuels on the fly. The flexible pipe from the valve to the injector can also be purged manually and was designed as short as possible. Each of the three tanks can be pressurised and depressurised separately and in case of an emergency shutdown of the engine a solenoid valve opens and all tanks are depressurised immediately.

### Camshaft Design

The design of the camshaft is responsible for the opening times of the inlet and exhaust valves. Between the F1/F2 and the F4 models the design differs significantly resulting in different opening times and overlap times (see Table 4.2) what in turn effects the quality of the gas exchange cycle.

	F1/F2	F4
I/O/IVC	10° ATDC / 34° ABDC	15° BTDC / 50° ABDC
EVO/EVC	40° BBDC / 15° ATDC	50° BBDC / 15° ATDC
Camshaft overlap	5°	30°

Table 4.2.: Difference in camshaft design and valve opening time.

The differences in valve timing and camshaft overlap between the two models is relatively

big and affects the rate of internal EGR rate. It can be assumed that the higher camshaft overlap causes a higher EGR rate, especially due to the earlier opening of the intake valve. The EGR rate decreases with lower compression ratios due to the higher dead volume. Though, the effect of higher pressures at higher compression ratios also affects the EGR rate and might even out the rate at different compression ratios.

EGR effects the temperature of the air/fuel mixture in two different ways. Firstly, EGR lowers the burnt gas temperature due to the inert effect of exhaust gas which in turn reduces the flame speed. Hence,  $\text{NO}_x$  emissions decrease with increasing EGR rate. In contrast unburnt hydrocarbons increase due to the lower flame speed and thus a higher flame quenching with increasing EGR rate. Secondly, due to the higher temperature of the burnt gas, EGR increases the charge temperature. Thus, an increasing EGR rate raises the affinity for knock.

### Valve Design

Figure 4.3 shows the differences in intake valves between the F1/F2 and the F4 model. The F1/F2 model, the standard engine for RON determination, has a 180 degree shroud on the intake valve which is supposed to create higher turbulences within the combustion chamber and therefore a better mixing. In contrast, the F4 model has a plane intake valve without any shrouds what changes the turbulences in the combustion chamber significantly. On the one

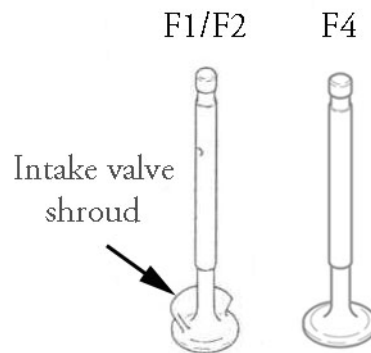


Figure 4.3.: Comparison of intake valves between the CFR F1/F2 model (left) and the CFR F4 model (right).

hand, higher turbulences lead to a faster combustion of the mixture, thus leaves the mixture less time for reactions prior combustion. On the other hand the higher rate in combustion leads to a higher pressure and temperature which has a negative effect on knocking.

These are the major factors identified in the design of the two models which affect the results in octane rating. In the following section effects due to changes beside the engine itself are presented.

### 4.1.2. Engine upgrade

Beside the differences in engine models described in the previous section several adaptations to achieve constant test conditions had to be made and are described in the following section.

#### Cooling System

The engine's head is cooled by a circulating coolant system with the coolant inlet temperature being automatically controlled. A solenoid valve in the building water line is actuated by a PID controller in order to control the building water flow. Heat is exchanged between the coolant and building water by means of a heat exchanger. In comparison, the standard rating engine is equipped with a convectively-driven cooling system in which nucleate boiling of the coolant maintains the cylinder head at 100 °C and a condenser extracts the resulting steam. As the coolant pump limited the coolant temperature to be not higher than 80 °C it was maintained at 75 °C (coolant inlet) respectively 81 °C (coolant outlet).

In general, a lower process temperature results in a lower tendency for knock. Further the difference in coolant temperature affects the heat transfer through the walls and enhances flame quenching at the walls. The effect of the difference in temperature on knocking is hard to quantify and depends on the the design of the engine. However, according to Pischinger [22] a coolant temperature lower by 10 K advances the knock limiting spark timing by 1 CAD.

#### Intake Air-Heater

The air delivery system is a closed loop system (house air) with the air flow controlled by critical orifices whereas the standard engine for octane rating is a naturally aspirated engine. The air pressure has to be adjusted manually to atmospheric pressure by means of a pneumatic precision regulator installed upstream of the heater. A pressure sensor determines the absolute pressure in the air line installed downstream the air heater. A compensating reservoir to damp oscillations in the air line is installed downstream the heater.

The MON standard defines the intake mixture temperature to be 149 °C. Hunwartz [15] claims that alcohol MON tests with the standard CFR equipment is not possible and published a way to modify a CFR test engine unit to determine octane numbers of alcohols correctly. The heater in the CFR engine is installed downstream of the plenum. To achieve the desired mixture intake temperature Hunwartz [15] suggests to install a heating element on the intake manifold. Due to the given intake manifold design this was not possible, hence adaptations of the engine test unit in order to perform MON tests could not be completed.

## Detonation Meter

The standard test engine is equipped with an electronic detonation meter that displays the knock intensity detected by a magnetostrictive-type transducer placed in the cylinder head [9]. The transducer gives a signal that is proportional to the rate of change of cylinder pressure. In the used engine no detonation meter was installed. Instead, a piezoelectric pressure transducer gives a signal proportional to the in-cylinder pressure. Knocking can either be observed audible or by examining the pressure trace visually. Additionally a knock intensity display was realised in LabVIEW. The used method is similiar to the energy knock detection method used by Breccq et al. [7] (cf. Chapter 6.1) but less accurate.

Syrimis et al. [28] scrutinised the effect of the spark plug and pressure transducer location on knock detection. They observed, that a pressure transducer located in a pressure node will record a smaller amplitude of fluctuation than a pressure transducer located farther from the pressure node. However, a signal with a smaller amplitude requires less data smoothing or filtering what consequently leads to a higher accuracy of the results obtained from the pressure data, e.g. the heat release rate or burn rate.

## 4.2. Measurement System

The engine's speed was measured by the means of an optical encoder installed on the crankshaft. A BEI H25 optical encoder triggers aquisition from a Kistler 6052B miniature piezoelectric pressure transducer every 0.1 crank angle degrees. The analog pressure transducer signal is first amplified by a Kistler type 5044 charge amplifier and then sampled by a Kistler data aquisition board.

Temperatures of the exhaust gas and the inlet mixture temperature were constantly measured by means of K-type thermocouples and recorded. Further the coolant temperature and the oil temperature were measured and displayed in LabVIEW.

Unfortunately no measuring device was available for detecting the mass of fuel consumed (fuel meter). It was tried to derive the mass of fuel consumed from the opening time of the injector valve. Therefore the volume the injector injected over a minute at a certain engine speed was measured in a graduated cylinder. With this reference it was the mass of fuel was calculated from the recorded opening times under different engine speed. However, it was discovered that this is not an appropriate mean to determine the mass of fuel consumed.

### 4.2.1. In-Cylinder Pressure Measurement

Typically, pressure indication is used to measure the in-cylinder pressure. A Kistler 6052B miniature piezoelectric pressure transducer was used. The transducer is installed by means of an adapter in the bore originally made for the detonation meter (see Figure 4.2).

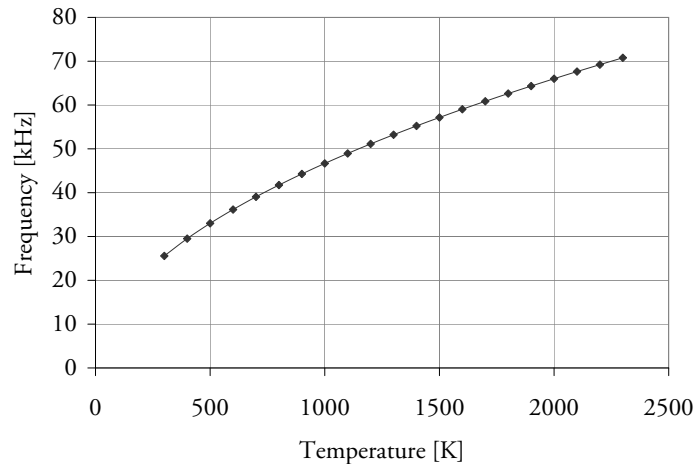


Figure 4.4.: Calculated frequencies for the used pressure transducer setup.

The transducer was mounted with an adapter in the cylinder head. This setup caused pipe oscillations what complicated the analyses of pressure data especially at higher compression ratios and entailed a more precise observation. The frequency of the pipe oscillation can be approximated with the following equation [1]

$$f = \frac{\sqrt{\kappa RT}}{2\pi} \sqrt{\frac{r^2 \pi}{Vl}} \quad (4.1)$$

where  $f$  denotes the frequency,  $\kappa$  the ratio of specific heat capacities,  $R$  the gas constant,  $T$  the temperature,  $r$  the radius of the indicating bore,  $l$  the length of the indicating bore and  $V$  the volume between the measuring surface of the pressure transducer and the top of the indicating bore. Figure 4.4 shows the frequencies in respect to temperature for the used pressure transducer and adapter setup. With the lowest frequency of 25.56 kHz at 300 K, the band-pass filter used in the frequency analysis filtered the pipe oscillations from of the signal.

### 4.3. Data Aquisition (DAQ)

The analog signal from the pressure transducer was conditioned by a Kistler type 5044 charge amplifier which compensates thermal drifts. The signal was then converted from analog to digital by a LabVIEW data acquisition board. The software developed by National Instruments, LabVIEW 8.5, was used as the graphical environment for data aquisition.

## Sampling Frequency

The encoder resolution of 0.1 CAD leads to a sampling frequency of  $f_s = 36$  kHz at 600 rpm and  $f_s = 54$  kHz at 900 rpm, octane tests and performance tests respectively. Syrimis et al. [28] reported that a sampling frequency of at least 50 kHz (1000 rpm) is required in order to detect the onset of knocking and the high frequencies occurring. They further reported, that a higher frequency than necessary leads to digitisation errors in light knocking cycles, hence the quality of the signal deteriorates.

To avoid an aliasing effect the Nyquist-Shannon sampling theorem was respected. The theorem states that any frequency higher than the half of the sampling frequency may not be reconstructed accurately. As long as this theorem is considered no aliasing effect will incidence.

## 4.4. Emission Measurement

Exhaust gases are sampled from the engine through a heated hose. To avoid that any vapour gets to the gas analyser, water was extracted from the exhaust gas by condensation in an ice bath. LabView was used to acquire readings from the gas analyser.

### Flame Ionization Magneto–Pneumatic Analyzer

The FMA-220 total hydrocarbon analyzer measures the total hydrocarbon concentration (FIA) as well as the oxygen concentration (MPA). The total hydrocarbon concentration is measured using a flame ionization detector whereas the oxygen concentration is measured with a magneto-pneumatic condenser microphone system. Figure 4.5 shows the basic prin-

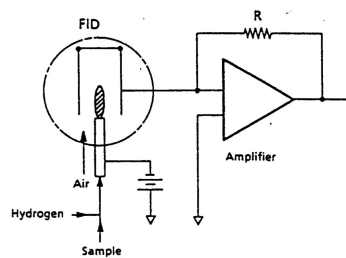


Figure 4.5.: Operating Principles of the Hydrogen Flame Ionization Detector<sup>c</sup>.

<sup>c</sup>Horiba Instruments INC., *Instruction Manual for FMA-220 FIA-220/MPA-220 Flame Ionization Magneto-Pneumatic Analyzer*, 1990.

ciple of the hydrogen flame ionization detector. If a hydrocarbon is exposed to a hydrogen flame it causes the tip of the jet nozzle to undergo ionization. On two sides of the flame an electrode is placed and a DC voltage is applied between the two electrodes. The ionization

causes a flow of ions between the electrodes which is proportional to the number of carbon atoms.

### Infrared Analyzer

The Horiba AIA-210 infrared analyzer uses a non-dispersive infrared analysis for constant measurement. Figure 4.6 shows the basic principle of the infrared analyzer. Infrared light emitted by a light source is converted into intermittent light by a chopper. The intermittent light passes the measurement cells (sample and reference cell) and enters the detector cell. In the measurement cell infrared light is absorbed by what causes a difference in intensity between the two beams entering the detector cell. This difference causes a membrane, located between the two detector cells, to vibrate and the changes in capacity between the electrodes for the membrane generates an electric output. Each component absorbs a specific infrared wavelength to which the detector is set but there is no response to any other wavelength. Hence, a change in infrared absorption means a change in concentration of a component.

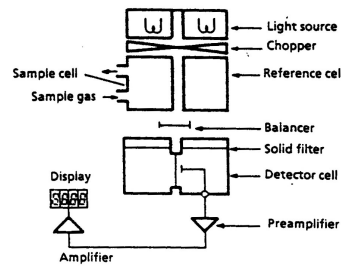


Figure 4.6.: AIA measurement – Infrared Analyzer<sup>d</sup>.

<sup>d</sup>Horiba Instruments INC., *Instruction Manual for AIA-210/220 Infrared Analyzer*, 1991.

### Chemiluminescent Analyzer

A Chemiluminescent Analyzer is used to measure  $NO$  and  $NO_x$  concentration in the exhaust gas. For the  $NO$  determination  $NO$  and  $O_3$  are mixed in a reaction chamber what effects a chemiluminescent reaction. Thereby light is emitted directly proportional to the concentration on  $NO$ . Silicon photodiodes sense the emitted light.  $NO_x$  is determined by the same principle except that prior the entry into the reaction chamber  $NO_2$  is first dissociated to  $NO$ .







## 5. Experimental Procedure

The differences between the standard engine for octane rating and the available engine were described in the previous section. Consequently, the standard experimental procedure for octane rating could not be applied and a new standard test procedure had to be established.

### 5.1. Fuels

All different used alcohols were available as neat components at high purity and had to be mixed manually before they were introduced to the fuel tanks. Further, all primary reference fuels had to be mixed in the same way. Therefore a standard graduated cylinder with a resolution of 10 ml was used to measure the required volume. Most mixtures of fuels were made out of neat components but also left-overs from a certain mixture were used and additional components were added in order to get the desired mixture ratio.

#### Primary Reference Fuels

In the octane number range of  $\text{RON} = 70 \div 100$  primary reference fuels as described in the ASTM standard were used. For octane numbers higher 100 so-called toluene standardisation fuels (TSF) were used as primary reference fuels. The ASTM standard defines a mixture including tetra-ethyl lead for octane numbers higher 100 but as tetra-ethyl lead was not available toluene standardisation fuels had to be used. Table 5.1 shows the composition of the reference fuels.

RON	n-Heptane	Iso-Octane	Toluene
$70 \div 100$	$(100 - \text{RON})\%$	RON %	
103.3	11%	15%	74%
107.6	6%	20%	74%
113		26%	74%

Table 5.1.: Composition of reference fuels.

MixedAlcohol fraction	Stoichiometric Air Requirement	LHV [MJ/kg]	LHV <sub>m</sub> [MJ/m <sup>3</sup> ]
0%	14.51	43.5	3.39
5%	14.26	42.7	3.38
10%	14.00	41.9	3.37
15%	13.75	41.2	3.37
85%	10.19	30.5	3.27
100%	9.43	28.2	3.26

Table 5.2.: Properties of different MixedAlcohol–Carbob blends. Lower heating value of stoichiometric air/fuel mixture (LHV<sub>m</sub>) at: T=300 K, p=1 bar.

## Alcohols

Only primary higher alcohols were used in this thesis. The composition of MixedAlcohol was as following: 75% ethanol, 11% propanol, 8% butanol and 6% pentanol (see Table 1.1). MixedAlcohol was used as a blending agent in Carbob in different blending levels shown in Table 5.2.

## 5.2. Resarch Octane Number (RON)

The ASTM D2699 standard [9] is the directive to follow in the determination of RON. Fundamental to all methods in octane number determination is that they compare the knock characteristic between a blend with a defined octane number, so-called primary reference fuels (PRF), and the knock characteristic of the sample fuels. Primary reference fuels are mixtures of n-heptane (RON = 0 by definition) and iso-octane (RON = 100 by definition) and by blending n-heptane and iso-octane in different volumetric mixture ratios, reference fuels with octane numbers in the range of 0–100 can be made. E.g., 20 vol.% n-heptane and 80 vol.% iso-octane result in a primary reference blend with an octane number of 80. For octane numbers greater 100 toluene is added as a third component. Specific volumetric mixture ratios to create reference fuels with octane numbers of 103.3, 107.6 and 113, are defined.

The most important test conditions defined in the standard for RON testing are summarised in Table 5.3. All the conditions beside the cylinder jacket temperature and the oil temperature were achieved. The cylinder jacket coolant was kept at a temperature of  $81 \pm 2$  °C (coolant out) and the oil temperature achieved a temperature of  $44 \pm 2$  °C. As all tests were conducted under the same conditions, the error in octane number determination was assumed to be small. In the following section the ASTM D2699 standard test method for RON determination is summarised before the used procedure is introduced.

Engine Speed	$600 \pm 6 \text{ min}^{-1}$
Spark Timing	$13^\circ \text{ BTDC}$
Intake Air Temperature	$52 \pm 1 \text{ }^\circ\text{C}$
Cylinder Jacket Coolant	$100 \pm 1.5 \text{ }^\circ\text{C}$
Oil Temperature	$57 \pm 8 \text{ }^\circ\text{C}$
Load	Wide open throttle
MAP	Naturally aspirated

Table 5.3.: Abstract of Standard operating conditions according to ASTM D2699.

### 5.2.1. The ASTM D 2699 Standard Test Method for Research Octane Number of Spark-Ignition Engine Fuels [9]

The standard provides guide tables presenting specific relationships between cylinder height (compression ratio) and octane number for specific primary reference fuels at standard knock intensity, tested under standard operating conditions. The term standard knock intensity (K.I.) refers to setting the air/fuel ratio where maximum knock intensity is identified, changing the cylinder height according to the guide table and adjusting the detonation meter to produce a mid-scale knockmeter reading of 50 for these conditions. Furthermore, a table to set the cylinder height to the barometric pressure compensated value for the octane number is provided.

#### Engine Standardisation

The engine is supposed to be running on standard engine settings (see Table 5.3) and temperature equilibrium for approximately one hour to ensure equilibrium operating conditions. The engine should be operated at a typical K.I. level for the last 10min. A toluene standardisation fuel (TSF) blend is used to qualify the engine as fit-for-use. The fit-for-use standardisation procedure differs for the octane range of the sample fuel. A specific procedure for octane numbers in the range of  $87.1 \div 100$  and one procedure for octane numbers below 87.1 and above 100. Basically, the procedures differ in terms of TSF blend composition and the rating range and therefore the rating tolerances.

#### Procedures

In the ASTM D2699 standard three different test methods are standardised, labeled Procedure A to C. All methods are based on the same standard engine operating conditions (see Table 5.3).

**Procedure A – Bracketing Procedure – Equilibrium Fuel Level** An engine fit-for-use test with a TSF blend applicable for the octane range and achievement of standard K.I. has to be performed before the sample fuel is introduced. Once the engine is running on the sample fuel the cylinder head has to be adjusted to cause a mid-scale knock meter reading. After this the air/fuel ratio has to be adjusted where highest knock intensity occurs. Equilibrium fuel level means “making manually incremental step changes in carburetor fuel level, observing the equilibrium knock intensity for each step and selecting the level that produced the highest knock intensity reading” [9]. This is followed by adjusting the cylinder height so that the knockmeter reading is  $50 \pm 2$  divisions. Two reference fuels are needed whereas one should have a lower and the other one a higher O.N. than the sample fuel, hence bracketing the sample fuel within the two reference fuels. Reference fuel no. 1 (higher O.N.) then is introduced, the air/fuel ratio adjusted for maximum K.I. and the knockmeter reading recorded. The same procedure has to be done with the reference fuel no. 2 (lower O.N.). All the three fuels have to be tested a second time but in the order sample fuel, reference fuel no. 2 before reference fuel no. 1 and both test results have to be in a certain tolerance value.

**Procedure B – Bracketing Procedure – Dynamic Fuel Level** This procedure is quite similar to the Bracketing Procedures - Equilibrium Fuel Level described above but it is restricted to O.N. within a range of 80 to 100 O.N. Dynamic fuel level means “introducing the fuel to the fuel reservoir, running the engine on this fuel whereas the fuel level in the fuel reservoir falls causing the mixture to change from rich to lean mixture at constant rate” [9]. The knock intensity rises to a maximum and decreases whilst an observation of the maximum knockmeter reading is possible. The fuel reservoir has to be refilled to the level with maximum K.I. Then the knockmeter reading and the compression ratio must be recorded. The same procedure has to be done with reference fuel no. 1 (higher O.N.) before reference fuel no. 2 (lower O.N.). The test procedure has to be repeated but the testing order changes to sample fuel, reference fuel no. 2 and reference fuel no. 1 at last.

#### Calculation of O.N. for Bracketing Procedures

The octane number of the sample fuel is determined by a linear interpolation (cf. Equation 5.1 [9]) with the recorded knock intensity of the sample and reference fuels and the octane numbers of the reference fuels.

$$O.N._S = O.N._{LRF} + \frac{K.I._{LRF} - K.I._S}{K.I._{LRF} - K.I._{HRF}} (O.N._{HRF} - O.N._{LRF}) \quad (5.1)$$

with the index  $S$  denote sample fuel,  $LRF$  lower reference fuel and  $HRF$  higher reference fuel.

Engine Speed	$600 \pm 6 \text{ min}^{-1}$
Spark Timing	$13^\circ \text{ BTDC}$
Intake Air Temperature	$52 \pm 1 \text{ }^\circ\text{C}$
Cylinder Jacket Coolant	$81 \pm 2 \text{ }^\circ\text{C}$
Oil Temperature	$44 \pm 2 \text{ }^\circ\text{C}$
MAP	$1.013 \pm 0.0025 \text{ bar}$
Injection time	TDC
Load	Wide open throttle

Table 5.4.: Operating conditions in the applied DON–procedure.

**Procedure C – CR Procedure** This procedure is only applicable for octane numbers within the range of 80 to 100. An engine fit–for–use test with an appropriate TSF blend for the expected sample fuel octane number range has to be done. Standard K.I. has to be achieved using a PRF blend with an octane number close to the expected octane number of the sample fuel. After introducing the sample fuel the cylinder height has to be adjusted to cause a mid-scale knockmeter reading. Then maximum knock intensity has to be determined by changing the fuel level in the fuel reservoir until knockmeter reading peaks. With the float reservoir set to the fuel level that produced maximum knock intensity the cylinder height has to be adjusted to obtain standard knock intensity reading recorded for the applicable PRF blend. Engine equilibrium is then upset by opening the carburetor’s drain valve. After closing the drain valve the knockmeter reading has to return to the previous knockmeter reading and the cylinder height setting is recorded and converted to O.N. with the appropriate guide table.

### 5.2.2. The Applied Procedure

Differences in equipment between the standard octane rating engine and the used engine (cf. Chapter 4) demanded a suitable test procedure. The established procedure differs significantly from the standard method for RON determination. For this reason the term RON is not used for the results but the term determined octane number (DON) is used instead.

In all different experiments the main focus was on achieving constant and equivalent conditions. This seemed to be the main factor in being able to compare results from different octane number tests. The operating conditions for the DON procedure are summarised in Table 5.4 which differ from the standard operating conditions defined by the ASTM D 2699 standard (cf. Chapter 5.2).

### **Engine Calibration**

In order to get the engine to steady state conditions a run-in period is crucial. The engine was motored for at least 15 min whilst the air-heater was already warming up the air. Then the fuel delivery system and the ignition was turned on so that the engine was firing. The engine was fired with standard gasoline for at least 30 min or until the oil and air reached the desired temperature, what mostly took longer. As the house air system was shut off every night the intake air pressure had to be readjusted by the pressure regulator to atmospheric pressure. Once this was achieved the ignition and fuel injection was turned off and a calibration of the engine at two arbitrarily chosen compression ratios was conducted. At compression ratios of 6.16 (MR = 0.6 inches) and 5.19 (MR = 0.8 inches) engine parameters like the manifold absolute pressure (MAP), in-cylinder pressure and intake temperature were checked against previous days. A reference day was defined to which the numbers from the calibration were compared to.

### **Engine Standardisation**

Much emphasis was put on minimising the influence of day to day variations. Therefore, as mandatory in the ASTM D 2699 standard, an engine fit-for-use test was conducted. This was done by logging a CR-sweep with gasoline at compression ratios in the verge of knocking to low knocking. The data was analysed and compared to data from a reference day. Perceptible variations were considered in the analysis of the data, thus a shift of numbers by the variation value.

### **Compression Ratio Sweep**

At all compression ratios, the engine was operating at a stoichiometric air/fuel ratio and wide open throttle. Starting at a low compression ratio, pressure traces were recorded of 100 consecutive cycles 4 times in a row, following in 400 consecutive cycles at one operating point. At low compression ratios (no knocking) the compression ratio was gradually increased by  $\approx 0.05$  inches in micrometer reading whereas at the verge of knocking steps were lowered to  $\approx 0.025$  inches in micrometer reading in order to gain a higher resolution at start of knocking. The compression ratio was increased until audible knocking was observed. At high compression ratios, steps were lowered to 0.01 inches in micrometer reading. Pressure traces were logged at each CR after the engine had run on this CR for at least 3 minutes. Motoring traces were taken before and after the sweep.

### **Determining Octane Number**

All recorded data was analysed using the method described in Chapter 6.3.

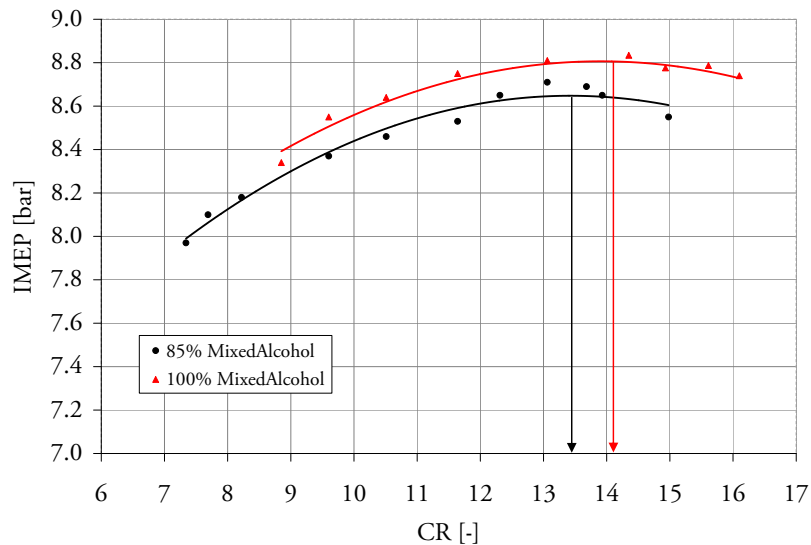


Figure 5.1.: Characteristics of performance at different compression ratios of two different MixedAlcohol blends.

### 5.3. Performance Tests

To show the potential of the MixedAlcohols a test procedure to achieve the performance in respect to the compression ratio was established. The indicated mean effective pressure ( $IMEP$ ) was used in the analyses of the data as the indicating value for performance. Both, a compression ratio and spark timing sweep was conducted whilst the engine was running at a stoichiometric air/fuel ratio and wide open throttle. Starting at a low compression ratio spark timing was advanced from no knocking to moderate knocking. Steps in spark timings were 2.5 CAD whilst the compression ratio was increased by steps of 0.05 inches in micrometer reading. Three times in a row, 100 consecutive cycles were recorded at each operating point. A dynamometer torque reading was recorded and also displayed the performance whilst operating. However, the objective of this sweep was to determine the best compression ratio spark timing combination for non-knocking combustion out of a fitted curve (see Figure 5.1).

Figure 5.1 shows the characteristics of the  $IMEP$  under different compression ratios with spark advance at the verge of knocking. Two different mixtures are shown and the arrow indicates the maximum in the fitted curve. Hence the best-compression-ratio-spark-timing combination, so-called best point compression ratio ( $BPCR$ ). Characteristically, the  $IMEP$  shows first an increase with increasing compression ratio to a maximum followed by a decrease in  $IMEP$  with increasing compression ratios. A second order polynomial curve was fitted to the data points and the compression ratio with the highest  $IMEP$  was derived from the graph. On a single day all different alcohol blends were tested in a spark timing sweep just at the

Engine speed	900 min <sup>-1</sup>
Intake air temperature	50 ± 1 °C
MAP	1.013 ± 0.0025 bar
Coolant temperature	75 ± 3 °C
Crank case oil temperature	48 ± 3 °C
Injection timing	TDC
Spark timing	Best point

Table 5.5.: Operating conditions for performance tests.

best point compression ratio in which the spark timing was varied in small steps (1 CAD) from non-knocking to moderate knocking. Finally, the performance of the different blends was calculated and compared. The basic operating conditions for the performance tests are summarised in Table 5.5. The operating conditions differ to the octane rating conditions in engine speed, in spark timing and in the slightly higher oil temperature (due to the higher engine speed). The engine speed was chosen to be 900 1/min following the standard test method for motor octane number determination. However, alcohols are sensitive fuels which have an advantage at lower engine speeds. Their high latent heat of vaporisation has a higher cooling effect on the mixture, hence reducing the process temperature. This effect is reduced at higher engine speed due to less time available for vaporisation and should therefore better demonstrate the performance of alcohols.

## 5.4. Emission Tests

Emissions were solely taken at the best point determined in the performance tests where the engine was operating at a stoichiometric air/fuel ratio and wide open throttle. Before emission data were recorded the engine was operating for at least two minutes under steady operating conditions whereas the sample pump of the Horiba gas analyser was on all the time. Emission data were recorded for at least 10 seconds, equivalent to data from 150 consecutive cycles.



## 6. Analysis Methods

The analyses of the data and methods to evaluate if knocking combustion occurs are presented in this chapter. MATLAB was used as the tool to numerically analyse data and to calculate different indicating numbers presented in the following chapters. For the lack of any professional software or any other code for the analyses of in-cylinder pressure data, all code had to be written. The code is not printed in this thesis but will be on the CD which is included in the back of this thesis.

### 6.1. Overview of Knock Detection Methods

Knock represents the limit for spark ignition engines on performance and efficiency. As already mentioned in Chapter 1 the compression ratio is a decisive factor for the efficiency of an engine. The detection of abnormal combustion onset is crucial for a smooth operation of an engine and can avoid major damage caused by knocking combustion.

In the following a brief overview over published methods for detecting knocking combustion are presented. According to Millo et al. [21] knock detection methods can be categorised according to the physical quantity they use to detect knock, as listed below:

- Methods based on cylinder pressure analysis
- Methods based on engine block vibration
- Methods based on gas ionisation analysis
- Methods based on heat transfer analysis

Most automotive applications use a method based on engine block vibrations detected by a low cost acceleration sensor to identify knock. The necessity of expensive pressure transducers for each cylinder limits the use of methods based on cylinder pressure analysis to research applications. As the indicated cylinder pressure is arguably one of the most accurate methods to detect knock, and the pressure data were recorded, only methods based on the analysis of the pressure data were studied.

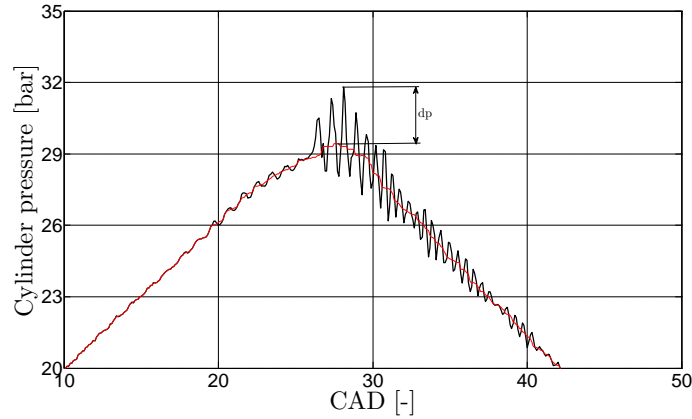


Figure 6.1.: Pressure oscillations in a knocking cycle.

### Single Pressure Value

Knocking pressure traces differ from non-knocking pressure traces in the sharp pressure peak and the typical fluctuating pressure curve mostly beginning shortly before the point of peak pressure. Knock detection methods based on the direct pressure signal analysis mostly use the maximum amplitude of pressure oscillations as the criteria (cf. Figure 6.1).

The red line in Figure 6.1 is the filtered pressure trace. The maximum difference in filtered pressure trace and raw data is defined as the maximum amplitude of pressure oscillations  $\Delta p_{\max}$  [19]. By applying this procedure to a certain number of cycles an evaluation on whether an operating point knocks or not is possible. Therefore a threshold value equal the limit for start of knocking has to be set. This value must be derived from pressure data studies and experience with the engine.

A comparison of maximum amplitudes between different operating conditions is shown in Figure 6.2. In the first row the spark timing is set to 13 CAD but the compression ratio is varied (RON test). In the second row the compression ratio is maintained constant whereas the spark timing is varied. As expected, the maximum pressure oscillations increase with rising compression ratio. This can also be observed in the second row, where the amplitude of pressure oscillations increases with increasing spark advance. Furthermore, the absolute value of the amplitude is lower in the first row as the compression ratio is lower. Moreover, the figure shows the strong dependency of the maximum amplitude of pressure oscillations on the operating conditions.

A widely used statistical method to define knock is that a certain number of cycles must exceed a critical threshold value  $\Delta p_{\max}$ . To demonstrate the behaviour of  $\Delta p_{\max}$  in respect to the compression ratio the 95% quantile is used as an indicating number. The 95% quantile represents the value which 5% of all cycles exceed, regardless of the average. In other words,

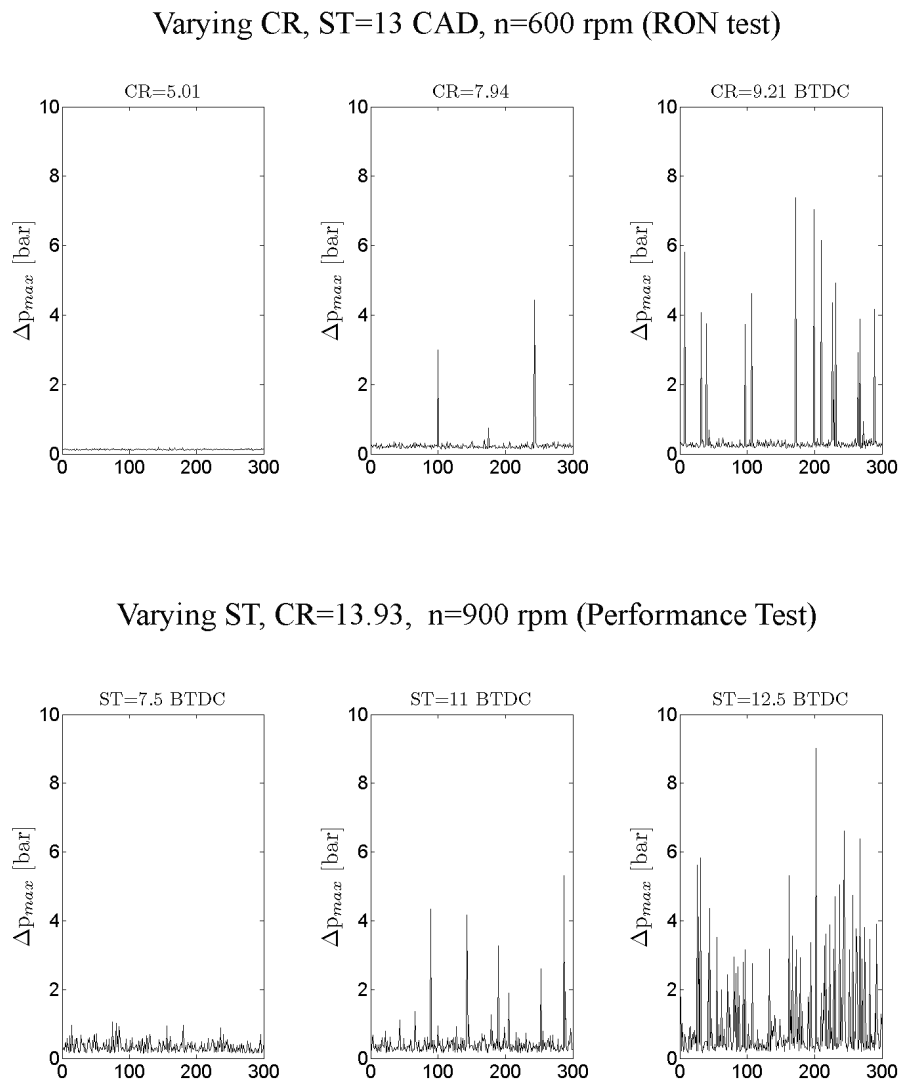


Figure 6.2.: Maximum amplitude of pressure oscillation under different operating conditions.

if 5% is the maximum number of knocking cycles allowed the 95% quantile is the  $\Delta p_{\max}$  that needs to be the maximum allowable pressure oscillation to detect less than 5% knock in the cycles.

### Pressure Derivatives

The gradient of pressure rise determined by the first derivative of the pressure is a widely used method for detection and control. Though the change in the pressure's first derivative is well related to the amount of the cylinder charge undergoing autoignition, the downside of the first derivative analysis is the several knock-independent factors which can affect the rate of pressure rise [21].

A knocking pressure trace differs from a non knocking pressure trace by the sudden increase in pressure (large positive curvature), a sharp pressure peak (large negative curvature) and the typical oscillating pressure (many changes in curvature). Since the curvature of a signal is determined by the second derivative, a rapid change in curvature would be associated with a large amplitude of the third derivative of the pressure trace. According to Gautam et al. [12], the maximum amplitude of the third derivative of the pressure trace could be considered as a knock indicator. An absolute threshold value to distinguish between a knocking cycle and a non knocking cycle has to be determined. This limit varies between engines and has to be specifically determined. It has to be based on the experience with the engine but also depends on the window of the pressure trace that is analysed. Lämmle [19] published that the major difference between a knock indicator derived by the third derivative to other techniques is, that it is applicable with data sampled at a low sampling frequency (1 CAD resolution) rather than requiring high sampling frequencies to resolve the typical knocking frequencies.

Figure 6.3 illustrates the differences between a non-knocking cycle (left) and a knocking cycle (right). The third derivative differs clearly between the two cycles. As already mentioned, the hardest part in this technique is to identify a threshold value to differentiate between knocking and non-knocking.

### Heat Release Rate Analysis

Another way of determining possible knock indicators is by a heat release analysis. The abnormal combustion in a knocking cycle causes according to Millo et al. [21] major shift in the heat release curve compared to a non knocking cycle. However, the computing time is high as each cycle has to be analysed and evaluated and a limit defining the start of knocking is rather difficult to determine.

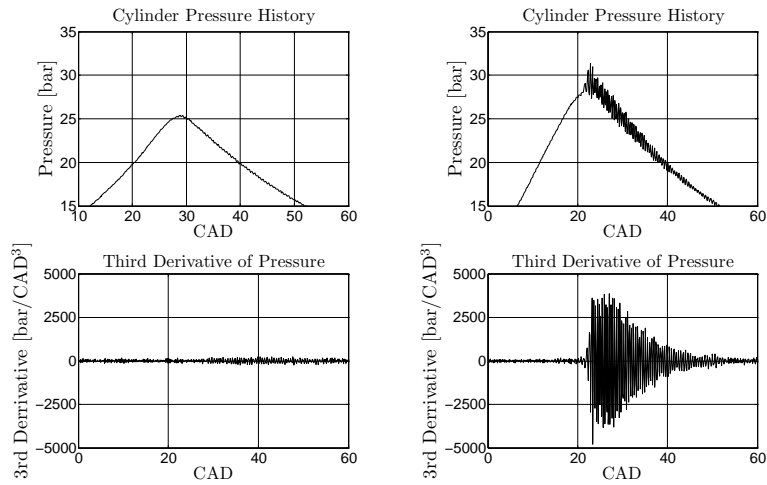


Figure 6.3.: Pressure trace and third derivative of propanol at 600 rpm,  $ST = 13$ : non-knocking (left),  $\varepsilon = 7.02$ ; knocking (right),  $\varepsilon = 9.21$ .

## Frequency Domain Methods

This often used method determines knock based on the high frequency pressure fluctuations that typically occur during knocking combustion. The amplitude is strongly linked to the amount of end-gas that undergoes autoignition. The chamber frequency has to be known and can be determined by solving the wave equation [24]. The signal then is band-pass filtered based on the calculated chamber frequency. One possible and often used way to derive a knock indicator is from the maximum pressure amplitude of the pressure oscillation. Each cycle is analysed and the maximum amplitude is compared to a predefined absolute threshold value that indicates knocking.

Brecq et al. [7] used an approach based on the energy of pressure oscillations. This method is based on the high frequency analysis of pressure oscillation and derives two indicators from this. Firstly, the so-called integral of modulus of pressure oscillations (*IMPO*) and secondly, the so-called maximum amplitude of pressure oscillation (*MAPO*). The pressure signal is first band-pass filtered, then rectified before the knock indicators are calculated. *IMPO* represents the energy contained in the high frequency oscillations of the cylinder pressure whilst *MAPO* looks at the maximum pressure oscillations due to knock. A more detailed description on *IMPO* is given in Chapter 6.2.

In this thesis focus is only on methods based on cylinder pressure analysis. In the following chapters basic principles and ways of knock detection based on cylinder pressure analysis are explained.

## 6.2. Used Knock Detection Methods

In this study the so-called Integral of Modulus of Pressure Oscillation (*IMPO*) published by Brecq et al. [7] is used for detecting knock. Figure 6.4 shows the procedure of how the *IMPO* is determined. The pressure signal is first band-pass filtered (4-10 kHz) to the chamber frequency, then rectified before being integrated over a certain window.

$$IMPO = \frac{1}{N} \sum_{N=1}^N \int_{ST}^{ST+W} |\tilde{p}| d\theta \quad (6.1)$$

Equation 6.1 shows the mathematical expression of the *IMPO* whereas  $N$  represents the number of cycles,  $ST$  the spark timing,  $W$  the width of the computational window and  $|\tilde{p}|$  is the filtered and rectified pressure signal. For this study a 90 CAD window was used. Several pressure traces were studied in order to determine the best window width. Especially at higher compression ratios where pipe oscillations interfered the signal, an accurate study of the pressure traces was essential.

Brecq et al. [7] published this method with a highpass filtering of the signal prior to rectification and integration. Highpass filtering is insufficient for the needs as oscillations in the pressure signal due to pipe oscillations occurred. These had to be filtered out of the pressure signal. Hence, the method published by Brecq et al. was adapted by using a band-pass filter instead of a high-pass filter to extract all frequencies not deriving from knock.

### Knock Frequency Analysis

The primary knock frequencies of a combustion chamber are determined by the diameter of the cylinder. Secondary knock frequencies are controlled by other dimensions of the combustion chamber, high level harmonics, and the downward motion of the piston. The chamber frequencies can be determined by solving the wave equation [24]. Different numbers for the chamber frequency are published in the range from 5–7 kHz [10] or 4–9 kHz [12].

A fast Fourier transformation was applied in order to determine the frequency components of the pressure signal (cf. Figure 6.5). Several cycles at different operating conditions were analysed and the frequency where the maximum amplitude occurred memorised and compared

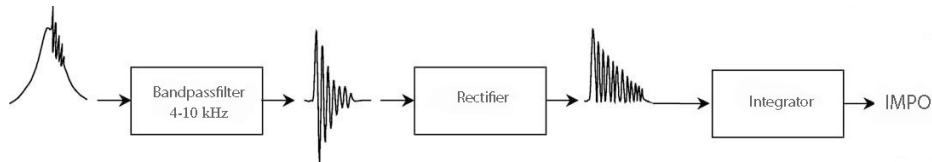


Figure 6.4.: Sketch of *IMPO* determination [7].

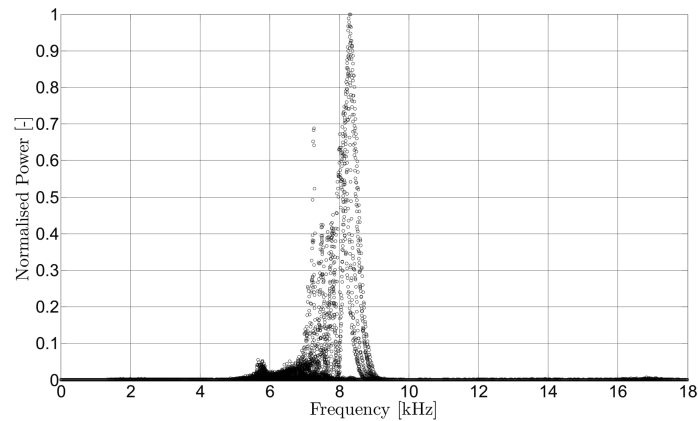


Figure 6.5.: Knock frequency analysis of a knocking operating point: Propanol, CR = 9.60, ST = 13.

against each other. This frequency was found to be in the same range for all cycles, namely between 4.5 kHz by lowest and 9.5 kHz by highest. Based on this finding the cut-off frequencies for the band-pass filter were set to 4–10 kHz. This finding confirms the expectation that the frequency of knock is equal to the resonant frequency of the combustion chamber.

### 6.3. Determination of Octane Number

To show the antiknock resistance of the different alcohols and alcohol blends a DON-test-procedure, as described in Chapter 5.2.2, was conducted. The IMPO and the third derivative of the pressure trace were used as characteristic values for knock detection.

Figure 6.6 shows the typical characteristic of the *IMPO*; it steadily increases with rising compression ratios until a certain compression ratio where the slope of the *IMPO* suddenly increases. This is the compression ratio where knocking combustion starts. A compression ratio sweep under motoring conditions was recorded and the *IMPO* calculated. The straight line represents the *IMPO* of the motoring data whereas the *IMPO*-value was shifted manually to a higher level. The linear equation of the motoring line was derived using Microsoft Excel. The shifted motoring *IMPO* represents the critical-*IMPO* to distinguish between knocking and non-knocking combustion. For all tested fuels the *IMPO* was calculated at each sampled data point before an evaluation, if the critical-*IMPO* was exceeded or not, was done. Each *IMPO* represents a mean *IMPO* derived from 400 consecutive cycles. The percent in *IMPO* exceeding was calculated resulting in a number representing the percentage of knock. This was plotted over the compression ratio whereas a curve was fitted in (see Figure 6.7). From this graph the critical compression ratio (CCR) was determined. Reason for displaying the percentage of knock was a simplification in defining the critical compression ratio. Primary reference

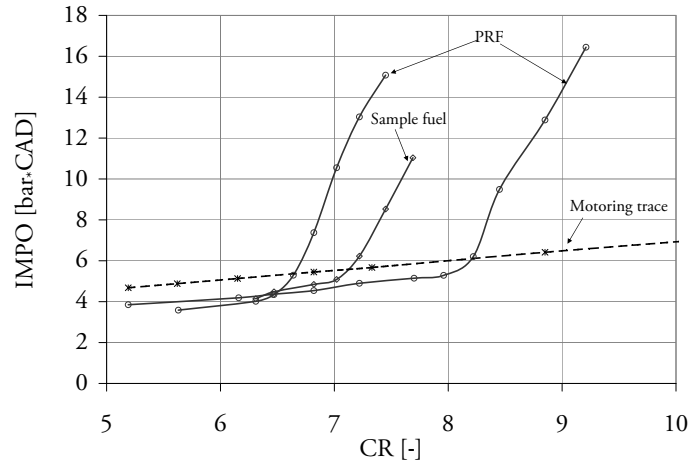


Figure 6.6.: Behaviour of the *IMPO* over compression ratio and the intersection of the *IMPO* with a motoring trace.

fuels with known octane numbers were analysed in the same way. The octane number was then calculated by a linear interpolation. From the graph (see Figure 6.7) the two reference fuels bracketing the sample fuel was found. With the known critical compression ratio of the three fuels and the known octane number of the two reference fuels, the octane number of the sample fuel was determined by a linear interpolation.

## 6.4. Performance Analysis

The indicated mean effective pressure (*IMEP*) was used as an indicating value for performance. In the analysis of the combustion event the net heat release rate as well as the mass fraction burnt rate were calculated. Two different methods were applied in the calculation of the mass fraction burnt, namely from the net heat release calculation and with the method established by Rassweiler and Withrow. Different indicating numbers like ignition delay, combustion interval or the crank angle where 50% of the charge was burned (*CA50*) were used to analyse the combustion under different conditions.

### 6.4.1. Indicated Mean Effective Pressure (*IMEP*)

The indicated mean effective pressure (*IMEP*) was used as an indicating value for performance and was calculated from the in-cylinder pressure data as shown in Equation 6.2 [10]. The indicated work is normalised by the swept volume in order to allow comparisons with other engines. For the calculation a mean pressure derived from 300 consecutive cycles was used.

$$IMEP = \frac{W_i}{V_s} = \frac{\int p_i dV}{V_s} \quad (6.2)$$



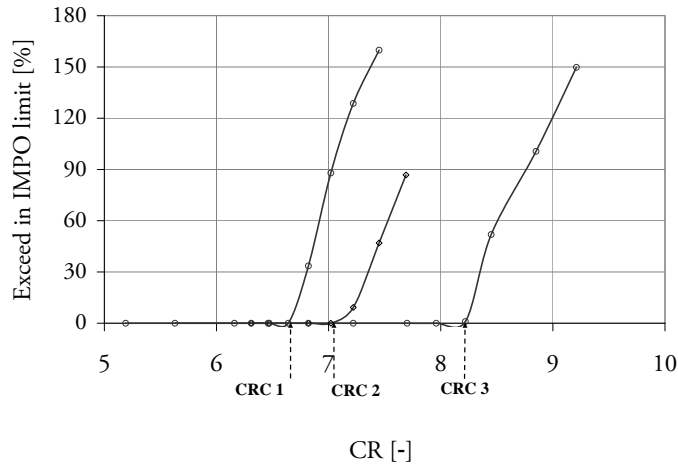


Figure 6.7.: Exceed in *IMPO* limit and critical compression ratios (CRC).

#### 6.4.2. Heat Release

The net heat release rate can be derived from the first law of thermodynamics and states the difference between the burn rate and wall heat losses. It is defined as [27]

$$\frac{dQ_{net}}{d\theta} = \frac{dQ_B}{d\theta} - \frac{dQ_W}{d\theta} = \frac{\gamma}{\gamma - 1} p \frac{dV}{d\theta} + \frac{1}{1 - \gamma} V \frac{dp}{d\theta} \quad (6.3)$$

where  $dQ_{net}/d\theta$  is the net heat release,  $dQ_B/d\theta$  is the burn rate,  $dQ_W/d\theta$  is the heat transfer with the chamber walls and  $\gamma=c_p/c_v$  is the ratio of the specific heat capacities. A detailed derivation of the heat release rate can be found in Appendix A.

Heat release analysis is the basic principle for determining the efficiency of a combustion event. In order to have a high efficiency the centre of gravity of the heat release curve, here defined as the crank angle where 50% of the bulk is burnt (CA50), has to be at an equilibrium in little heat transfer and low mechanical load. If CA50 is early in the expansion stroke, peak pressure and temperature rise. Therefore the heat transfer increases with temperature as  $NO_x$  emissions do and high pressures signify high mechanical load. Therefore CA50 has to be around  $8^\circ CA$  [31] or  $10\text{--}15^\circ CA$  [5] after top dead centre. Although the heat release analysis includes more approximations than the burn rate analysis, it has proven its ability whereas comparisons showed, that the centre of gravity between both methods disagrees in less than  $1^\circ CA$  [31]. The cumulative net heat release rate is calculated by an integration of the net heat release rate.

$$Q_{cum} = \int dQ_{net} d\Theta \quad (6.4)$$

Figure 6.8 shows both, the net heat release rate and the cumulative net heat release. The heat release analysis evaluates the data on a differential basis (equation 6.3) what leads to noise in the computed result [27].

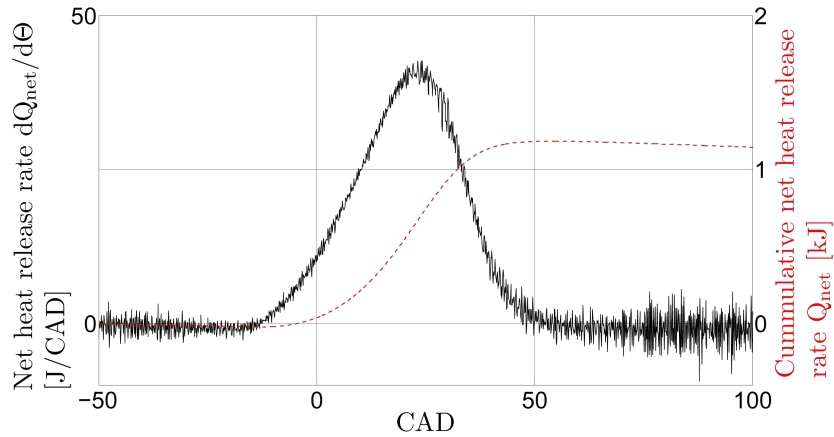


Figure 6.8.: Net heat release rate  $dQ_{\text{net}}/d\theta$  and cumulative net heat release rate  $Q_{\text{cum}}$ .

### 6.4.3. Mass fraction Burnt Analysis

The mass fraction burnt is a well established indicator in the analysis of combustion. It illustrates the speed of the combustion event and is therefore a good indicator for the efficiency of a combustion cycle. In the following two used methods to determine the mass fraction burnt are presented. Firstly, it can be calculated from the net heat release data and secondly, by using the model published by Rassweiler and Withrow. However, both methods were used to calculate the ignition delay (ID), the combustion interval (CI) and the crank angle, where a 50% fraction in mass of the charge is burnt (CA50). The ignition delay is defined as the crank angle interval between the start of combustion and the time when a small but significant fraction in mass is burnt. In this work the combustion interval is defined as the crank angle interval between spark timing ( $ST$ ) and 10% mass fraction burnt. The combustion interval is defined as the crank angle interval required to burn the bulk of the charge. In this work it is defined as the crank angle interval between 10% and 90% mass fraction burnt.

#### From the Heat Release Rate

Prior to the calculation of the mass fraction burnt the end of combustion (EOC) has to be determined. In this work the maximum of the cumulative net heat release rate was used as the crank angle for the end of combustion. End of combustion can also be defined as the crank angle where the net heat release rate first gets negative after the point of maximum heat release. Both ways lead to the same crank angle. Once EOC is determined the mass

fraction burnt can be calculated by [12].

$$mfb = \frac{\sum_{i=ST}^{\theta} (dQ_{net}/d\theta)_i}{\sum_{i=ST}^{EOC} (dQ_{net}/d\theta)_i} \quad (6.5)$$

### The Rassweiler and Withrow Method

The Rassweiler and Withrow method is a widely used technique to calculate the mass fraction burnt (mfb) [14]. The basic principle of this method is based on the assumption that the pressure rise during an encoder interval can be separated into a pressure rise due to combustion ( $\Delta p_c$ ) and a pressure change due to the variation in volume ( $\Delta p_v$ ) (cf. equation 6.6 and Figure 6.9).

$$\Delta p = \Delta p_c + \Delta p_v \quad (6.6)$$

The pressure change due to combustion  $\Delta p_c$  from  $p_i$  to  $p_{i+1}$  can be calculated by a polytropic process.

$$\Delta p_c = p_{i+1} - p_i \left( \frac{V_i}{V_{i+1}} \right)^n \quad (6.7)$$

The equation has to be normalised

$$\Delta p_c^* = \Delta p_c \frac{V_i}{V_{TDC}} \quad (6.8)$$

From this the mass fraction burnt (mfb) can then be calculated by

$$mfb = \frac{\sum_0^i \Delta p_c^*}{\sum_0^N \Delta p_c^*} \quad (6.9)$$

Whereas  $N$  is defined as the increments occurring after end of combustion and  $\theta$  as the spark timing.

This method is widely used and accepted, though it contains several approximations. On the one hand heat transfer effects can only be considered by the extent that the polytropic exponent  $n$  differs appropriately from the real ratio of specific heat capacities  $\gamma$  and on the other hand “the pressure rise due to combustion is proportional to the amount of fuel chemical energy released rather than the mass of mixture burnt” [14]. Further, the polytropic exponent  $n$  – as an adiabatic process is assumed – is equal to the ratio of heat capacities ( $c_p$ ,  $c_v$ ). Specific heat capacities are functions of temperature but vary little with temperature. Hence,  $n$  is assumed to be constant. The end of combustion is defined as the crank angle where the pressure rise due to combustion becomes zero [2], [3], [14], [27].

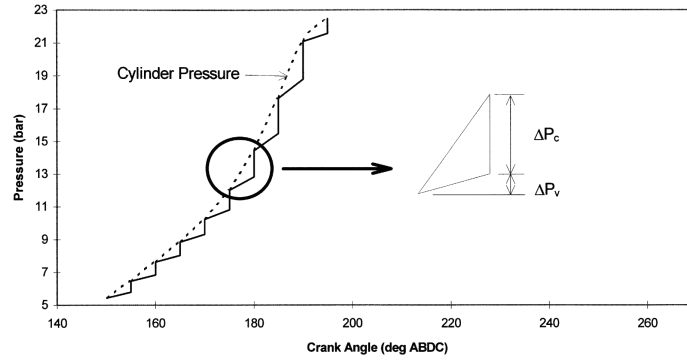


Figure 6.9.: Measured pressure change as a sum of piston motion and combustion [2].

Numbers derived from both methods were compared against each other. However, the derived indicating numbers between the two models were significantly less than 1 crank angle degree what proofed the applicability of both methods.

#### 6.4.4. Gas Temperature

The gas temperature can be found from the equation of state  $pV = mRT$ . The temperature was determined using both, the so called “Schnelles Heizgesetz – AVL” which is based on the ideal gas law as well as from the ideal gas law with the calculated mass of air/fuel mixture. In terms of the “Schnelles Heizgesetz – AVL” the required starting temperature at BDC was set to the manifold temperature (333 K). For the ideal gas law the determined mixture mass is based on calculation and not on accurate measurement (cf. Chapter 4.2) which can be a significant source of error. Calculating it in both ways enables a comparison of the methods but its greater value is the assessment of accuracy of the calculated fuel mass. However, both methods do not consider the vaporisation of the air/fuel mixture in the cylinder. This cooling effect is especially for blends with a higher alcohol concentration significant due to the distinctly higher latent heat of vaporisation of alcohols.

In the “Schnelles Heizgesetz – AVL” the equation of state is first used to define the constant  $1/mR$  by assuming the gas temperature at bottom dead centre (here referred with the index  $0$ ) before the compression stroke.

$$\frac{T_0}{p_0 V_0} = \frac{1}{mR} = \text{constant} \quad (6.10)$$

$T_0$  was assumed to be equal to the intake manifold temperature of 333 K. With the determined constant  $1/mR$  the gas temperature for the whole engine cycle can be determined from the equation of state:

$$T = \frac{pV}{mR} = pV \frac{T_0}{p_0 V_0} \quad (6.11)$$

Both methods were applied and compared against each other. The comparison showed a difference of 200 K what is attributed to the error in the mass of fuel. The “Schnelles Heizgesetz – AVL” seemed to be accurate enough in order to be able to compare gas temperatures against each other.

## 6.5. Emissions analyses

Emissions were analysed by a Horiba gas analyser whereas concentrations of unburnt hydrocarbons (*THC*), nitrogen oxides (*NO<sub>x</sub>*), carbon monoxides (*CO*) and carbon dioxides (*CO<sub>2</sub>*) were measured. Emissions data were analysed in both, cycle emissions (*ppm*) as well as brake specific emissions (*ppm/kWh*). To display the difference between different alcohol blends, emission data are presented relative to the emissions of Carbob, the non-oxygenated hydrocarbon fuel used as the base line for the MixedAlcohol blends.



## 7. Results

In this chapter the results of the experiments are presented. The composition of the different fuels tested can be found in Chapter 5.1.

### 7.1. Determined Octane Number

Table 7.1 shows the DON for neat alcohol components as well as the RON found in literature [6]. In terms of octane numbers for alcohols, published numbers vary significantly between different publications. A chart presenting the characteristic of the *IMPO* over compression ratio of all tested fuels, from where the knock limiting compression ratio was determined, can be found in Appendix C. The method with the Ethanol clearly showed the strongest resistance against knocking and a reasonable number could be determined. Butanol is in good agreement with the published RON. Standard gasoline showed a lower resistance against knock compared to the real RON. For pentanol, by far showing the lowest resistance against knock, no published RON could be found. But Baramik [4] mentions that Pentanol is known to decrease the RON when blended with standard Gasoline.

Fuel	DON	RON
Ethanol	112.79	106-130
Propanol	99.89	
Butanol	95.00	94
Pentanol	75.21	
Gasoline (AKI 91)	90.00	$\approx 95$
Carbob	82.38	87

Table 7.1.: Determined octane number (DON) of alcohols in comparison with RON found in literature.

Alcohols showed the expected behaviour; decreasing octane number with increasing number of carbon atoms or, in other words, decreasing octane number with increasing size of molecule. However, this behaviour is further displayed in Figure 7.1 and is also in agreement with the behaviour of alkanes presented in Chapter 2. The higher octane number of the MixedAlcohol

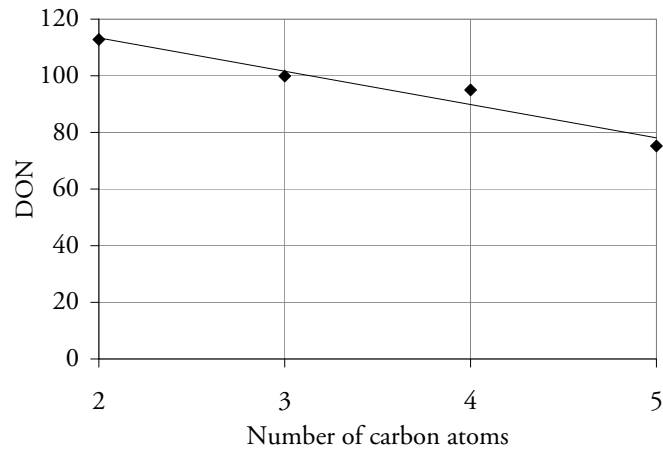


Figure 7.1.: Dependence of determined octane number DON on number of carbon atoms.

Fuel	KLCR	DON
Carbob	5.95	82.38
5% MixedAlcohol	6.02	83.21
10% MixedAlcohol	6.16	84.88
15% MixedAlcohol	6.47	88.19
85% MixedAlcohol	9.21	105.17
100% MixedAlcohol	10.51	110.63
Gasoline (AKI 91)	6.64	90.00
50%/50% Ethanol/Gasoline	9.14	104.88

Table 7.2.: Determined octane number of different blends.

blend compared to Carbob leads to the expectation of an increasing octane number with increasing blending level. This could be confirmed and is shown in Table 7.2 and Figure 7.2.

Figure 7.2 shows the determined octane number for the different blending levels. Also included in the graph is the determined octane number for standard gasoline (AKI=91). However, Chevron's standard gasoline contains 5.6% of oxygenates whereas solely ethanol is used. Carbob was supposed to be the base component for standard gasoline (AKI = 91) before adding 5.6% oxygenates. Ethanol is the main component of the MixedAlcohol blend (75%), thus ethanol mostly determines the thermophysical properties of the MixedAlcohol blend. Consequential, adding 5% MixedAlcohol to Carbob should result in the same octane number as standard gasoline. This could not be confirmed what leads to the assumption (by considering the error in octane number determination) that Carbob is actually not the base component for standard gasoline with an AKI of 91 but rather for standard gasoline with an AKI of



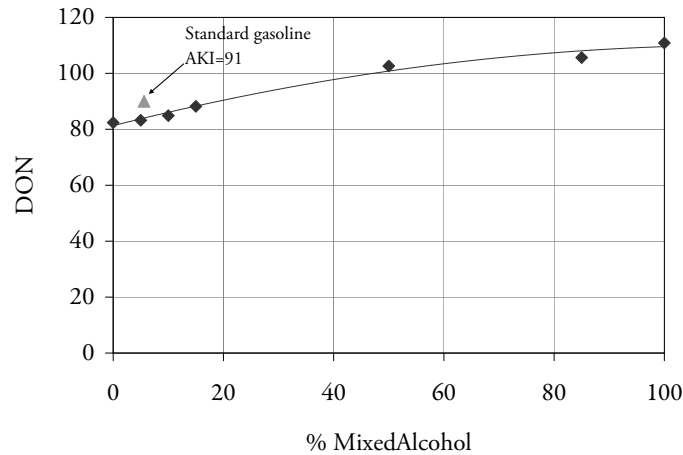


Figure 7.2.: Determined octane number of different MixedAlcohol blends.

87. Figure 7.3 shows the increase in knock limiting compression ratio relative to Carbob with increasing blending level. The compression ratio is crucial for the efficiency of the ideal standard Otto cycle  $\eta_i$  (cf. Chapter 1), thus operation at higher compression ratios increases the limiting thermal efficiency. However, at low blending levels the major component, Carbob, controls the knock resistance and prohibits a higher increase in compression ratio. Once MixedAlcohol becomes the main component (85% blend) in the blend the increase in knock resistance is significant. Standard gasoline showed an increase in KLCR of 11.6% relative to Carbob.

However, the test results show that with the developed DON-procedure an accurate RON-determination is not possible but rather an approximation of the real RON. The error in measurement and procedure can be shown by comparing DON and RON of Carbob and Gasoline. The difference between RON and DON for Carbob is 6.29 whereas the difference for Gasoline is 3.45. It seems that the procedure is less accurate at lower RON but is closer with the real RON at higher octane numbers (cf. Table 7.1). This tendency could also be shown in a different project conducted with different gasoline blends. It can just be assumed that both, the DON-procedure as well as the engines setup make a contribution to the error in octane number determination.

## 7.2. Performance Tests

The indicated mean effective pressure was calculated and used as a characteristic number to qualify the performance of the different blends. The performance of all MixedAlcohol blends as well as gasoline are shown in Figure 7.4. The determined combination of best compression ratio and spark timing, here called best point compression ratio (BPCR) is summarised in

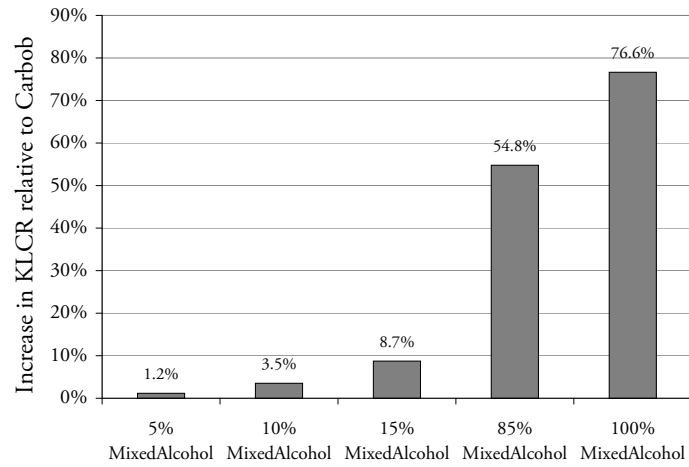


Figure 7.3.: Increase in knock limiting compression ratio (KLICR) relative to Carbob ( $\varepsilon = 5.95$ ).

	CR	ST
Carbob	6.02	25.0
5% Mixed Alcohol	6.84	17.5
10% Mixed Alcohol	6.82	20.0
15% Mixed Alcohol	7.23	17.5
85% Mixed Alcohol	13.06	12.5
100% Mixed Alcohol	14.35	11.0
Gasoline	7.69	17.5

Table 7.3.: Best combination of compression ratio and spark timing for different blends.

Table 7.3.

Expectedly, Carbob has the lowest performance whereas the 5% MixedAlcohol blend shows a higher *IMEP* at its best point but also a significantly lower performance at compression ratios unlike the best point. The 10% MixedAlcohol shows a higher *IMEP* but at a lower compression ratio than the 5% MixedAlcohol blend. The 15% MixedAlcohol blend follows the trend of a higher performance with increasing blending level at a higher compression ratio. However, the 5% blend shows an exceptional performance by showing the highest *IMEP* at a higher compression ratio than expected. The different behaviour of the 5% blend can also be seen in the heat release analysis. Based on the results from the octane number determination the increase in compression ratio is too high. This behaviour clearly shows, that performance is not necessarily just based on the octane number.

Gasoline (AKI = 91) has its best point at a higher compression ratio than the MixedAlcohol blends in the level 0–15%. This can be attributed to the low octane number of Carbob rather

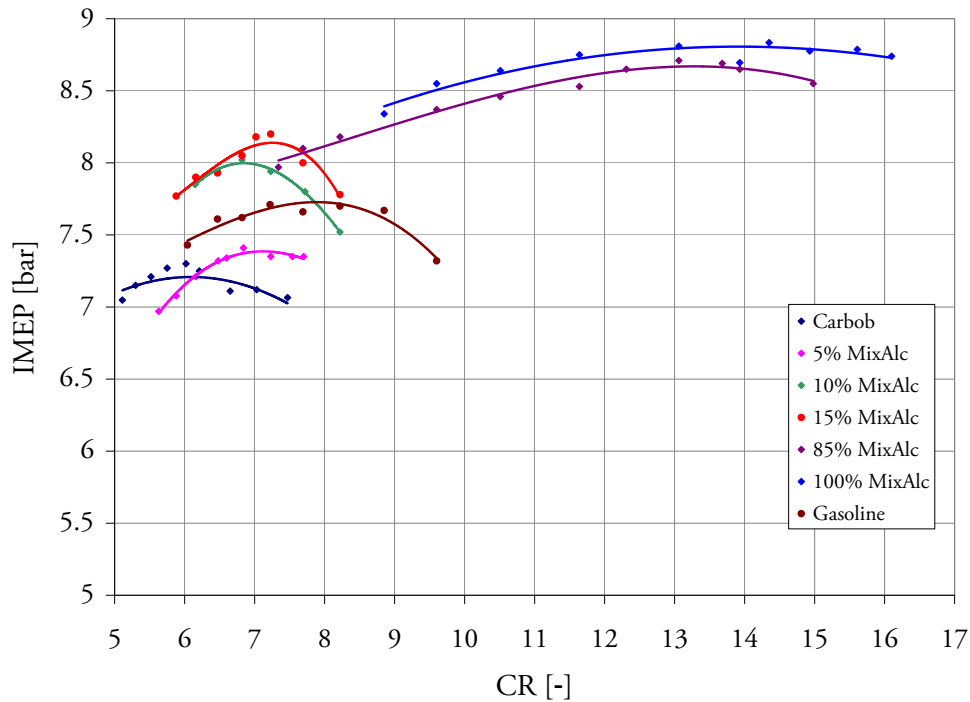


Figure 7.4.: Performance results of different fuels at BPCR.

than to a speciality of gasoline. Again, as already mentioned in the discussion on the octane number results (cf. Chapter 7.1), the 5% MixedAlcohol blend can not bear a comparison with gasoline. Though, by considering the much lower octane number of Carbob compared to gasoline, Carbob shows a similar but slightly lower performance in the best point.

A significant increase in BPCR can be seen for the 85% and 100% MixedAlcohol blend. Both blends show the same trend but differ in *IMEP* at their best points. Consistently, the higher octane number allows a higher compression ratio for the 100% blend but both blends perform over a wide range in compression ratio with an acceptable performance.

Except for the 5% blend, all low level blends show nearly the same curvature as Carbob. It is assumed, that because of the low fraction of MixedAlcohol the alcohols can not realise the potential it shows at higher blending levels. It was further observed that a certain fuel requires a certain compression ratio to show an improvement. This gets obvious by comparing the 15% and the 85% blend where the two curves intersect. The ON of both blends is significantly different but the performance is almost the same.

Figure 7.5 shows the increase in *IMEP* relative to Carbob with increasing blending level. The increase in *IMEP* is equal to an increase in output of an engine by keeping the speed of the engine and the swept volume constant. In The 5% MixedAlcohol blend showed only a small increase in performance but in the 10% and 15% blends, MixedAlcohol displayed their

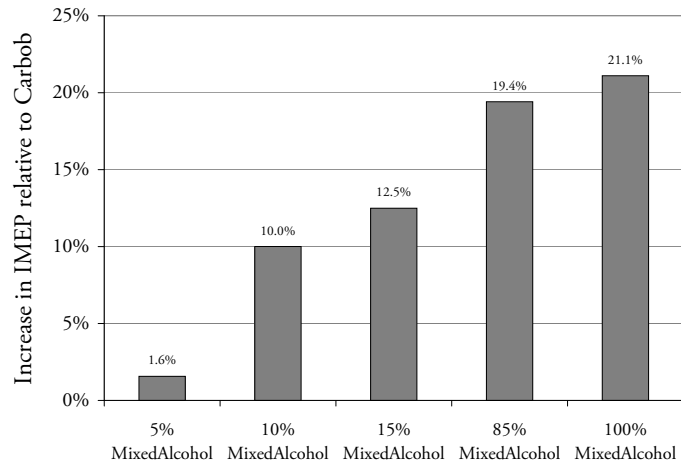


Figure 7.5.: Increase in *IMEP* relative to Carbob each blend operating at BPCR.

actual performance they also showed at blending levels of 85% and 100%.

### Effect of Engine Speed on Performance

The engine speed influences the knock limiting compression ratio positively. Mostly because of the higher turbulence at higher engine speed. Further, the combustion event occurs at higher *rpm* at roughly the same band of crank angle degree and the time for reactions prior to combustion is shorter. However, the differences in speed in the experiments conducted is not big ( $\Delta \text{rpm} = 300$ ) but the increase in KLCR is significant.

Figure 7.6 shows the differences in spark timing and compression ratio between 600 rpm and 900 rpm. The advance in spark timing compares spark timings at equal compression ratios. Here the KLCR defined in the octane number tests was used to compare spark timings at 600 rpm with the spark timings at 900 rpm. For the difference in compression ratio, the knock limiting compression ratios at 600 rpm and 900 rpm at equal spark timing of  $ST=13$  were compared. For example, the 85% MixedAlcohol blend started knocking at 600 rpm at  $CR=9.21$  whereas at 900 rpm the best point compression ratio is  $CR=13.06$  with a retarded spark timing of just 0.5 CAD. For lower level blends the increase in compression ratio is not as significant instead the difference in spark timing is. On the other hand, Carbob knocking was observed at  $CR=5.95$  whereas at 900 rpm the best point was at  $CR=6.02$ . This only means an increase in compression ratio of  $\Delta CR=0.07$  but the spark timing is 12 CAD retarded at 600 rpm. A tendency to both, a decreasing advance in spark timing at equal compression ratios with increasing blending level as well as an increase in compression ratio at equal spark timing with increasing blending level, could be observed. Though, a quantitative conclusion must not be derived from this comparison but it demonstrates the effect of engine speed.

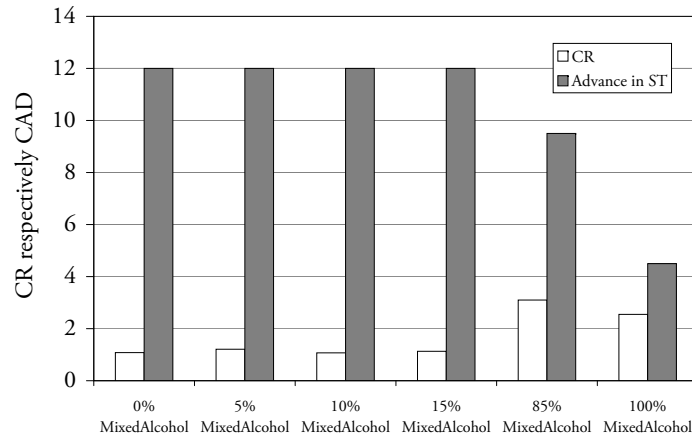


Figure 7.6.: Differences in spark timing and compression ratio at 600 rpm and 900 rpm.

### 7.2.1. Exhaust Gas and Burnt Gas Temperature

Figure 7.7 shows the exhaust gas and the adiabatic burnt gas temperature. Based on the increasing compression ratio with increasing blending level the burnt gas temperature rises with the blending level. In contrast, the exhaust gas temperature shows the opposite characteristic, namely a decrease in temperature with increasing blending level. This can be attributed to the lower compression ratio setting for lower level blends and therefore a less efficient operating point.

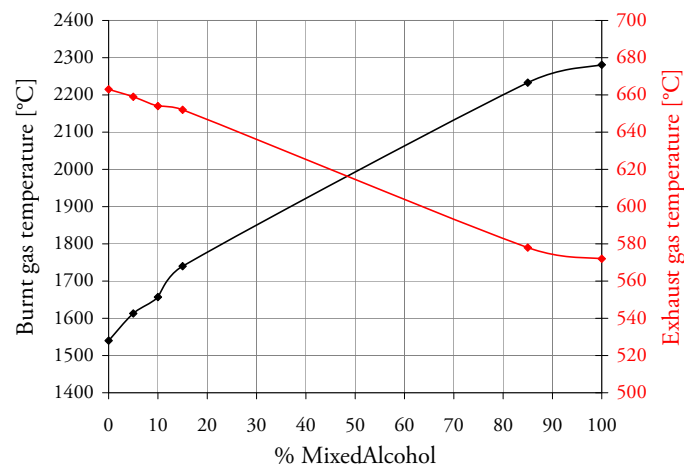


Figure 7.7.: Exhaust gas temperature and adiabatic burnt gas temperature operating at BPCR and full throttle position.

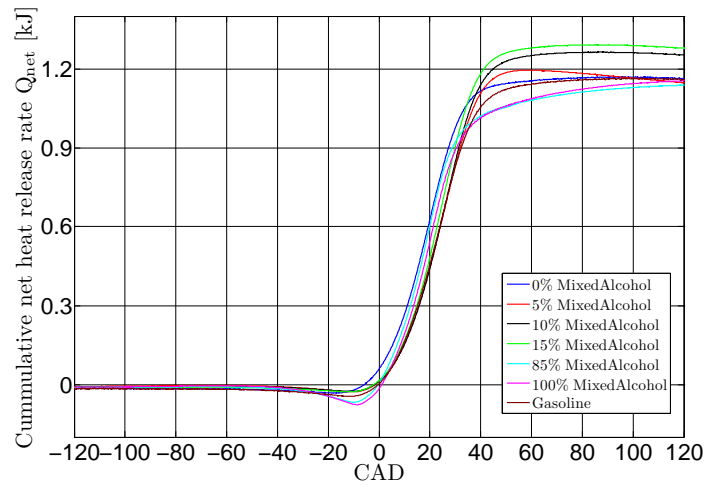


Figure 7.8.: Cummulative net heat release of different fuels operating at BPCR and full throttle position.

### 7.2.2. Net Heat Release Rate Analysis – Mass Fraction Burnt Analysis

Figure 7.8 shows the cumulative net heat release rate of all different MixedAlcohol blends as well as for gasoline. The negative heat release rate for the high level blends implies, that the heat transfer through the walls is higher compared to lower level blends where hardly any difference in the minimum net heat release rate can be seen. The increase of the heat transfer coefficient with increasing temperature causes a higher heat transfer rate. Higher compression ratios create higher temperatures (cf. Figure 7.7) what in turn causes the minimum cumulative net heat release rate to be lower. Though it has to be considered, that the ratio of specific heat capacities was kept constant ( $\gamma = 1.3$ ) for all different blends.

All different fuels beside the 5% blend showed a quite late end of combustion which is defined as where the net cumulative heat release rate has its maximum. It appears to be as late as  $120^\circ$  CA after top dead centre for the higher level blends. The ignition delay time (Figure 7.9) was observed to be almost constant at low blending levels but significantly shorter for high level blends. A quite similar characteristic, but not as distinct at high blending levels as the ignition delay characteristics, shows the combustion interval. A trend to a shorter combustion interval with higher fraction of MixedAlcohol can be seen. These characteristics can be attributed to a higher flame velocity of alcohols. The higher compression ratio causes higher in-cylinder pressures what lowers the speed of flame. The higher gas temperatures at higher compression ratios overcompensates the decrease due to pressure resulting in a higher flame speed.

In Figure 7.10 a comparison in mass fraction burnt of the low level blends under equal

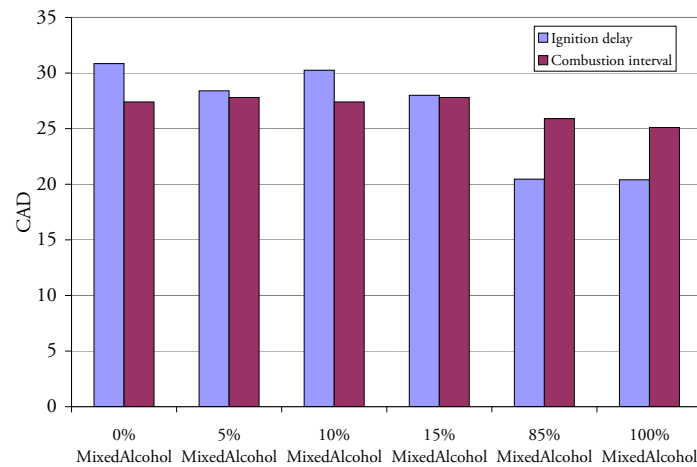


Figure 7.9.: Ignition delay ( $ID$ ) and combustion interval ( $CI$ ) of different blending levels determined at the best point of each blend.

operating conditions is shown. Noticeable is the significantly earlier end of combustion of the 5% MixedAlcohol blend and the quite late end of combustion of all other fuels. The significantly earlier end of combustion of the 5% MixedAlcohol blend could also be observed under different operating conditions. Like in the performance analysis shows the 5% MixedAlcohol blend a different behaviour. An explanation for this behaviour could not be found but is assumed to result due to exceptional chemical kinetics of this blend.

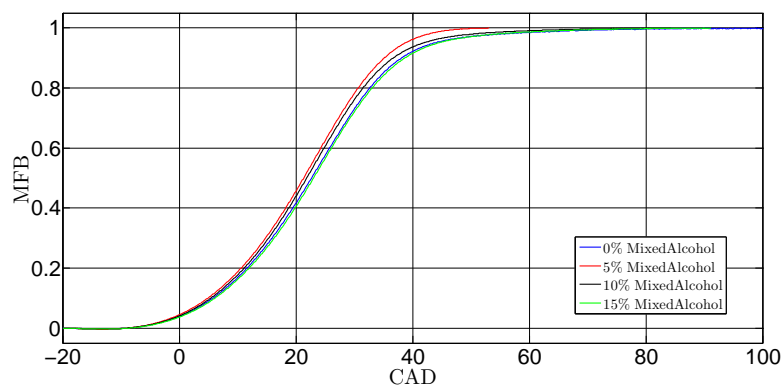


Figure 7.10.: Mass fraction burnt of different low level MixedAlcohol blends under equal operating conditions:  $CR=6.48$ ,  $ST=20$ .

Figure 7.11 shows the mass fraction burnt whereas hardly any difference can be seen between the 85% and the 100% blend. No substantial conclusion can be drawn from the mass fraction burnt analysis beside that the difference between the fuels is small and the differences do not follow a pattern.

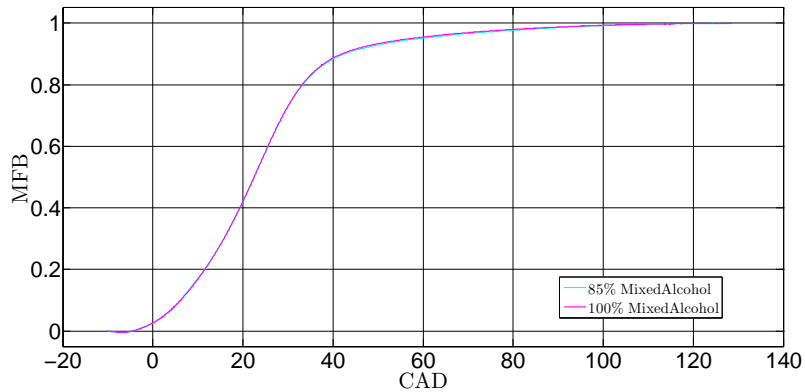


Figure 7.11.: Mass fraction burnt of high level MixedAlcohol blends under equal operating conditions: CR=13.06, ST=10.

### CA50 Analysis

The crank angle where 50% of the bulk is burnt is a good indicator to show the efficiency of an operating point. Figure 7.12 shows the CA50 of the different blending levels with the high level blends and Carbob at around 20 CAD. No obvious trend can be seen in the comparison of CA50 of different blends.

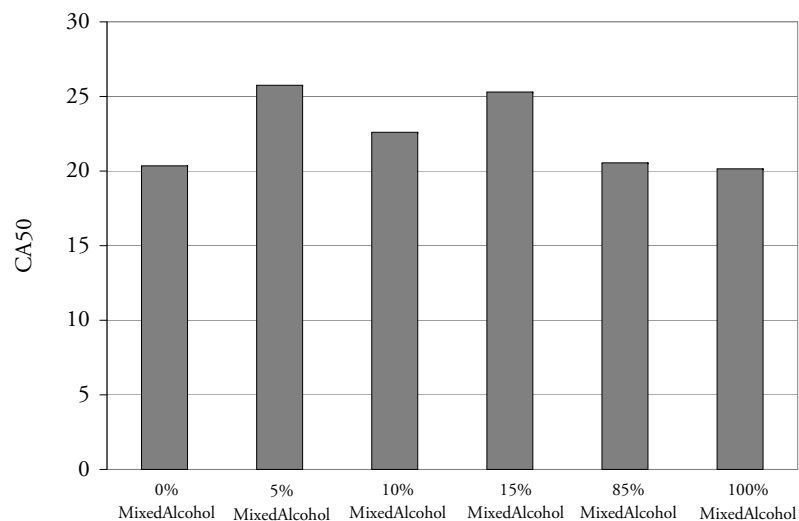


Figure 7.12.: Crank angle degree where 50% of the bulk is burnt (CA50).



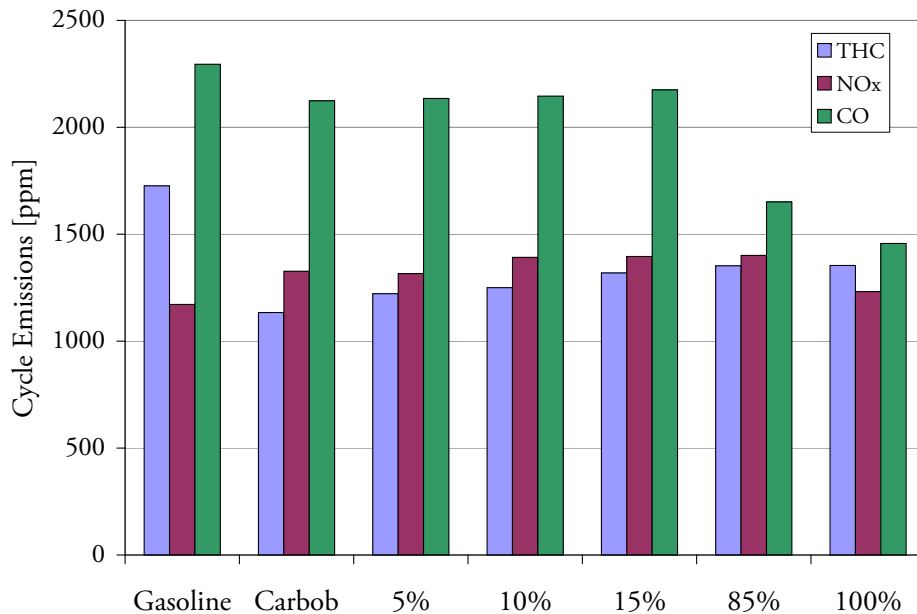


Figure 7.13.: Cycle emissions of different MixedAlcohol blends operating at their BPCR.

### 7.3. Emission Tests

Figure 7.13 shows the cycle emissions (THC, NO<sub>x</sub>, CO) for all different fuels tested in unit parts per million. This graph is supposed to give an idea of the engines exhaust gas composition but also to clarify the quantity in emission. Gasoline showed the highest emissions of all tested fuels in total hydrocarbons and carbon monoxide emissions but also the lowest in nitrogen oxid emissions.

Due to the age of the engine a comparison of the absolute emission numbers with a modern engine is absurd and a presentation of the absolute emission numbers would not help in the review of the emission results. Further the objective is to show the differences of different MixedAlcohol blends. Therefore, only the increase in emissions relative to Carbob are presented and discussed.

In the following chapter, emissions in terms per unit parts-per-millions (*ppm*) will be called cycle emissions and emission in terms per unit of parts-per-million per unit power output (*ppm/kW*) will be called brake specific emissions.

#### Total Hydrocarbon Emissions

The total hydrocarbon cycle emissions, shown in Figure 7.14, are significantly higher for all blends. Brake specific emissions are higher in low level blends and lower for high level blends. The characteristics of the cycle emissions can be attributed to the higher compression

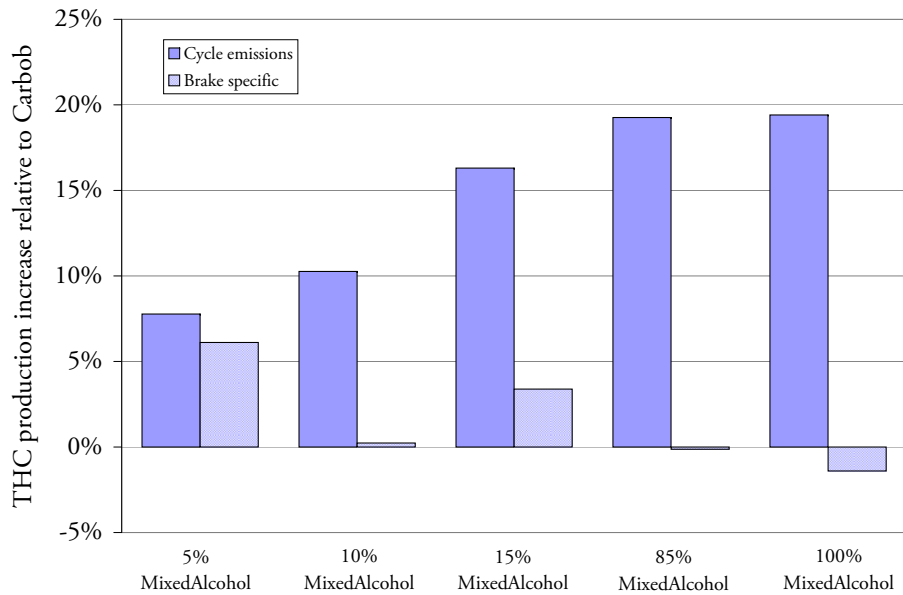


Figure 7.14.: Increase in THC emission relative to Carbob operating at BPCR.

ratios promoting more unburnt hydrocarbons in crevices. The speed of flame increases with increasing temperature and alcohol content. The higher flame speed leaves less time for the unburnt hydrocarbons to diffuse into the extinguishing flame and therefore more unburnt hydrocarbons survive. This characteristic is also in agreement with the combustion intervals presented in Chapter 7.2.2. However, worth mentioning is, that gasoline showed an increase of 45% in brake specific emissions and 52% in cycle emissions compared to Carbob.

### Nitrogen Oxide Emissions

The  $\text{NO}_x$  cycle emissions, shown in Figure 7.15, show an increase in  $\text{NO}_x$  emissions for the 10%, 15% and 85% blend. Instead, for the 5% blend a minor decrease and for the 100% blend a significant reduction can be seen. For the brake specific emissions a progressive reduction is shown ending in a reduction of 23% for the neat MixedAlcohol blend. As expected, an increase in  $\text{NO}_x$  emissions with increasing compression ratio, hence increasing gas temperature, is shown for all blends beside the neat MixedAlcohol blend. This is in agreement with the origin of Zeldovich- $\text{NO}$  explained in Chapter 3.4.1.

### Carbon Monoxide Emissions

The cycle emissions of  $\text{CO}$ , as shown in Figure 7.16, are almost equal for the low level blends and clearly lower for the high level blends. The brake specific emissions are lower for all blends

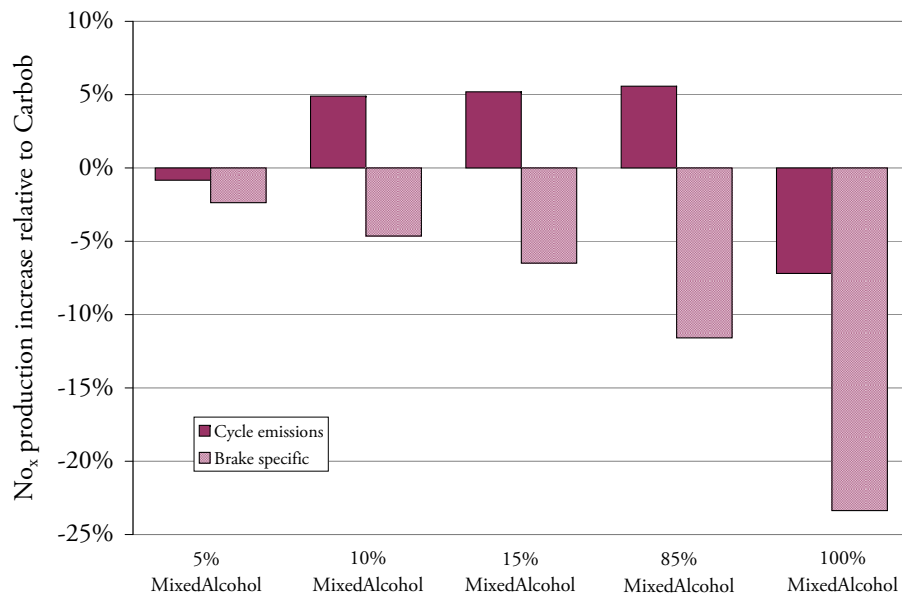


Figure 7.15.: Increase in  $\text{NO}_x$  emission relative to Carbob operating at BPCR.

and a reduction of more than 40% for the neat MixedAlcohol blend was observed. This can be attributed to the diluting effect resulting from consuming more mass of fuel as the alcohol content in the blend increases while maintaining a stoichiometric mixture strength.

### Overall Emissions

Figure 7.17 compares the production increase in THC,  $\text{NO}_x$  and CO brake specific emissions against each other. It can be summarised, that adding MixedAlcohols lowered  $\text{NO}_x$  and CO brake specific emissions for all different blending levels. A progressive decrease with increasing MixedAlcohol content was observed. In terms of THC emissions a clear trend is missing but for the 85% and 100% blend a decrease was observed.

Figure 7.18 compares the production increase in THC,  $\text{NO}_x$  and CO cycle emissions against each other. Most obvious are the higher THC emissions compare to Carbob. Beside the 85% blend in CO and the 100% blend in CO and  $\text{NO}_x$  no reduction in cycle emission could be observed.

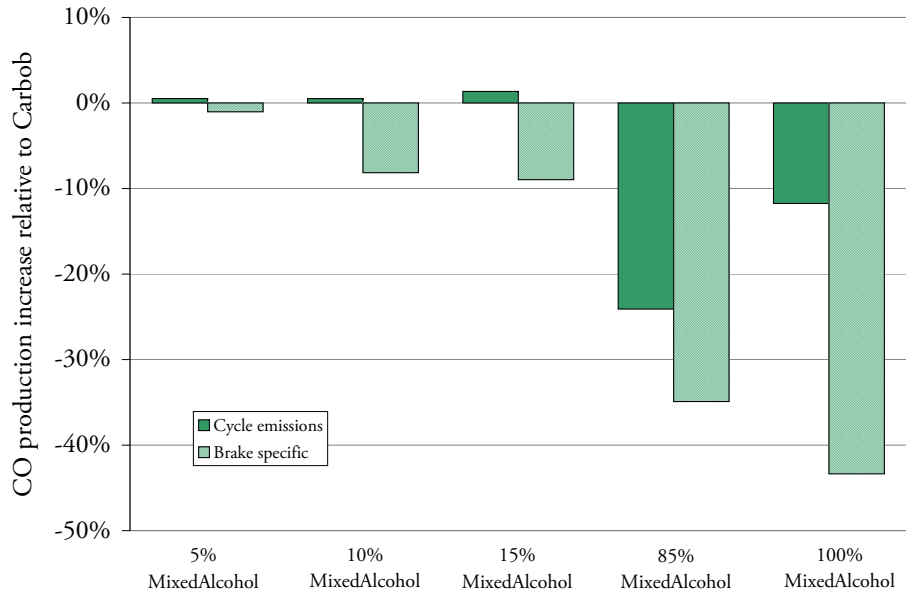


Figure 7.16.: Increase in CO emission relative to Carbob operating at BPCR.

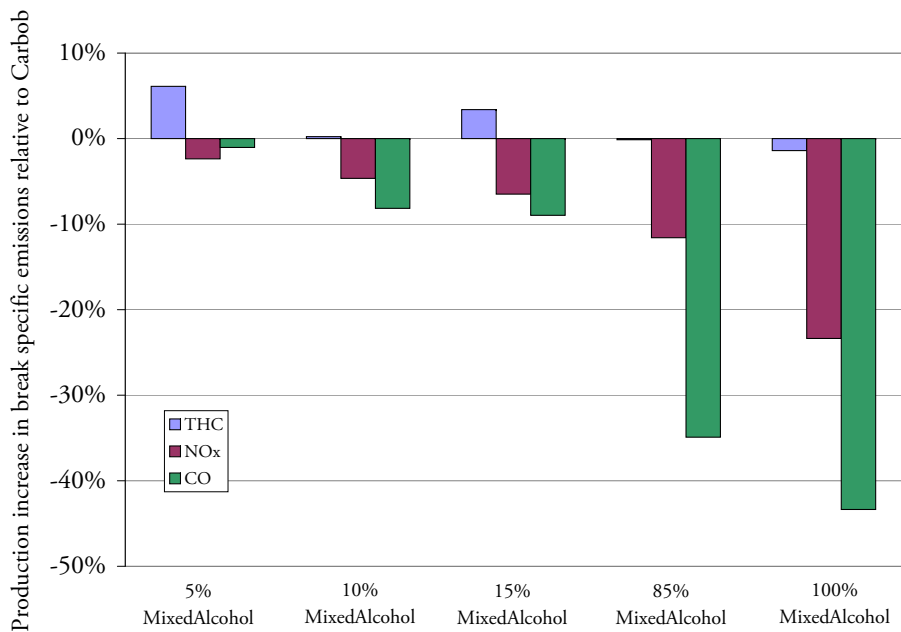


Figure 7.17.: Increase in brake specific emissions relative to Carbob operating at their BPCR.

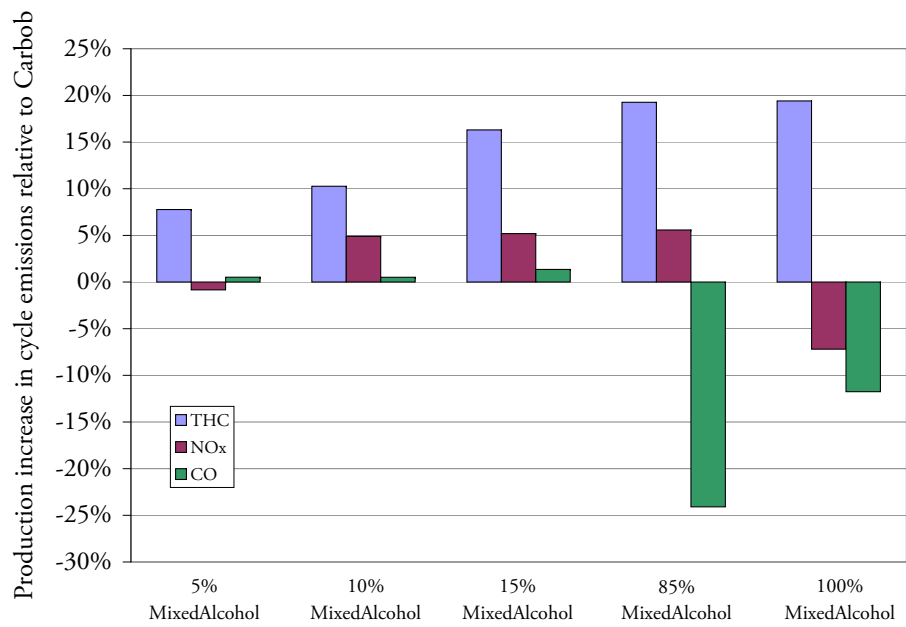


Figure 7.18.: Increase in cycle emissions relative to Carbob operating at their BPCR.



## 8. Conclusions and Future Work

For a successful campaign against global warming and climate change, biofuels are a promising option for the future. Fundamental to this, but not scope of this thesis, is a sustainable way of producing biofuels, what means, considering our climate and the humanitarian point of view. This thesis means a small step in the establishment of biofuels in our world.

### 8.1. Conclusion

The objective of this thesis was to determine the performance and emission characteristics of a higher order alcohol mixture (in this thesis called MixedAlcohol) derived from a thermochemical conversion of biomass to mixed alcohol fuel. Both, MixedAlcohol as a blending agent in non-oxygenated gasoline (so-called Carbob) as well as neat MixedAlcohol were tested. In order to simulate currently used blending levels, volumetric fractions of 5%, 10%, 15% and 85% MixedAlcohol in Carbob were tested as well as neat Carbob and neat MixedAlcohol; thus six different blends. No information on Carbob could be obtained and forced to draw up assumptions on different numbers required in thermodynamics.

The single cylinder research engine available for testing had to be adapted to the requirements of octane rating. After a two month period of repair, because of an engine seizure happened in October 2008, the whole test bench had to be adapted once the engine was running. The requirements defined in the ASTM standard for octane rating could, within the limits of the engine, partly be achieved. Differences in the engine setup – intake manifold injection instead of a carburetor, no detonation meter installed – are just the strongest distinctions between the required and the available engine setup. The engine's setup demanded the establishment of a new test procedure to determine octane numbers. The test procedure was applied and proved, that an approximation of the real octane number and a comparison of octane numbers determined with this method, is absolutely possible. However, comparison in the determined and real octane numbers showed, that it is not possible to accurately determine octane numbers. If an accurate octane number determination is desired both, an improvement of method is necessary, but above all, the setup of the engine has to conform to the standard.

Appropriate methods for the analysis of the data had to be found. The assessment if knocking combustion occurs, was a major part in this thesis for both, in octane number tests

as well as the performance tests. Therefore, a method based on the analysis of a certain band of frequencies in a pressure trace, was used. For an evaluation of this method, a second method using the third derivative of the pressure signal as an indicating number, was applied.

### Conclusion of the Test Results

- Octane numbers of ethanol, propanol, butanol and pentanol were determined. A comparison with numbers found in literature, confirmed the determined number. The octane number linearly decreases with the number of carbon atoms. Octane tests with the six different MixedAlcohol blends showed the expected performance of increasing octane number with higher blending levels.
- MixedAlcohols proved their ability in terms of performance. The output of the engine, in this thesis represented by means of the indicated mean effective pressure, was measured at the combination of compression ratio and spark timing resulting in the highest performance. An increase in performance with increasing blending level was observed whereas the neat MixedAlcohol blend showed an increase in IMEP relative to Carbob of 21%.
- Brake specific emission could be shown to reduce with higher blending fractions of MixedAlcohol. Adding MixedAlcohol lowered  $\text{NO}_x$  and CO brake specific emissions for all different blending levels, in which a progressive decrease with increasing MixedAlcohol content was observed. THC brake specific emissions were higher for the low level blends (5%, 10%, 15%) but lower for high level blends (85%, 100%).

In terms of cycle emissions no real improvement could be shown with unburnt hydrocarbon emissions being significantly higher at all blending levels. Nitrogen oxide emissions were lower just for the 5% and 100% blend and higher by approximately 5% for all other blending levels.

## 8.2. Future Work

Although the work presented in this thesis is of great value, there is still much work to be done in order to exploit the advantages of biofuels as fully as possible. I believe the most important next step is to test these fuels in an engine closer to a state of the art engine. This work showed the behaviour of MixedAlcohols at low engine speed and is a basis for further investigations. Testing these fuels on an engine equipped with technologies like direct injection or a variable valve-control system are possible ways to utilise the advantages of MixedAlcohols. In general, deploying the high latent heat of alcohols for an increase in volumetric efficiency, is a promising approach.



# Bibliography

- [1] AVL List Gmbh Austria. *Indizieren am Verbrennungsmotor: Anwenderhandbuch*, 2002.
- [2] J.K. Ball, R.R. Raine, and C.R. Stone. Combustion analysis and cycle-by-cycle variations in spark ignition engine combustion. part 1 : an evaluation of combustion analysis routines by reference to model data. *Proceedings of the Institution of Mechanical Engineers, Part D: Journal of Automobile Engineering*, 212(5):381–399, 1998.
- [3] J.K. Ball, R.R. Raine, and C.R. Stone. Combustion analysis and cycle-by-cycle variations in spark ignition engine combustion part 2: a new parameter for completeness of combustion and its use in modelling cycle-by-cycle variations in combustion. *Proceedings of the Institution of Mechanical Engineers, Part D: Journal of Automobile Engineering*, 212(6):507–523, 1998.
- [4] V.P. Barannik, V.V. Makarov, A.A. Petrykin, and A.V. Shamonina. Aliphatic Alcohols - Antiknock Additives to Gasolines. *Chemistry and Technology of Fuels and Oils*, 41(6):452–455, 11 2005.
- [5] R. v. Basshuysen. Motorlexikon. Website, August 2009. <http://motorlexikon.de/>.
- [6] G.L. Bormann and K.W. Ragland. *Combustion Engineering*. McGraw–Hill, 1st edition, 1998.
- [7] G. Brecq, J. Bellettre, and M. Tazerout. A new indicator for knock detection in gas si engines. *International Journal of Thermal Sciences*, 42:523–532, 2003.
- [8] J. Clar. Introducing Alcohols. Website, July 2009. <http://www.chemguide.co.uk/organicprops/alcohols/background.html#top>.
- [9] ASTM International West Conshohocken. *ASTM D 2699 - 06a Standard Test Method for Research Octane Number of Spark-Ignition Engine Fuel*, 2006.
- [10] H. Eichlseder. *Verbrennungskraftmaschinen - Vertiefte Ausbildung*. Institut für Verbrennungskraftmaschinen und Thermodynamik, 2005.
- [11] H. Eichlseder, M. Klütting, and W.F. Pioock. *Grundlagen und Technologien des Ottomotors: Der Fahrzeugantrieb*. Springer Wien NewYork, 2008.

- [12] M. Gautam and D.W. Martin II. Combustion characteristics of higher-alcohol/gasoline blends. *Proceedings of the Institution of Mechanical Engineers, Part A: Journal of Power and Energy*, 214(5):497–511, 2000.
- [13] Moscow Glushko Thermocenter, Russian Academy of Sciences. Entropy and heat capacity of organic compounds in NIST Chemistry WebBook, NIST Standard Reference Database Number 69, Eds. P.J. Linstrom and W.G. Mallard, National Institute of Standards and Technology, Gaithersburg MD. Website, March 2009. <http://webbook.nist.gov/>.
- [14] J. Heywood. *Internal Combustion Engine Fundamentals*. McGraw–Hill, 1st edition, 1988.
- [15] I. Hunwartz. Modification of CFR Test Engine Unit to Determine Octane Numbers of Pure Alcohols and Gasoline-Alcohol Blends. *SAE Paper 820002*, 1982.
- [16] Landolt-Börnstein. *Landolt-Börnstein - Group IV Physical Chemistry - Viscosity of Pure Organic Liquids and Binary Liquid Mixtures/ [edited by] Malcolm W. Chase Jr.* Springer, 25th edition, 1998.
- [17] W.R. Leppard. The Chemical Origin of Fuel Octane Sensitivity. *SAE Paper 902137*, 1990.
- [18] D.R. Lide. CRC Handbook of Chemistry and Physics. Website, March 2009. <http://www.hbcpnetbase.com/>.
- [19] C. Lämmle. *Numerical and Experimental Study of Flame Propagation and Knock in a Compressed Natural Gas Engine*. PhD Thesis, Swiss Federal Institute of Technology Zurich, 2005. Diss., Technische Wissenschaften, Eidgenössische Technische Hochschule ETH Zürich, Nr. 16362, 2006.
- [20] H. Menrad, M. Haselhorst, and W. Erwig. Pre-Ignition and Knock Behavior of Alcohol Fuels. *SAE Paper 821210*, 1982.
- [21] F. Millo and C.V. Ferraro. Knock in S.I. Engines: A Comparison between Different Techniques for Detection and Control. *SAE Paper 982477*, 1998.
- [22] F. Pischinger. Abschlußbericht Sonderforschungsbereich 224: Motorische Verbrennung. 2001.
- [23] R. Pischinger, M. Klell, and T. Sams. *Thermodynamik der Verbrennungskraftmaschine*. Springer Wien NewYork, 2nd edition, 2002.
- [24] D. Scholl, C. Davis, S. Russ, and T. Barash. The Volume Acoustic Modes of Spark-Ignited Internal Combustion Chambers. *SAE Paper 980893*, Februar 1998.

- [25] National Science, Committee on Environment Technology Council, and Natural Resources. Interagency Assessment of Oxygenated Fuels. June 1997.
- [26] T. Searchinger, R. Heimlich, R. A. Houghton, F. Dong, A. Elobeid, J. Fabiosa, S. Tokgoz, D. Hayes, and T. Yu. Use of U.S. Croplands for Biofuels Increases Greenhouse Gases Through Emissions from Land-Use Change. *Science*, 319(5867):1238–1240, 2008.
- [27] R. Stone. *Introduction to Internal Combustion Engines*. Society of Automotive engineers, Inc. Warrendale, Pa., 3rd edition, 1999.
- [28] M. Syrimis and D.N. Assanis. Knocking Cylinder Pressure Data Characteristics in a Spark-Ignition Engine. *Journal of Engineering for Gas Turbines and Power*, 125(2):494–499, 2003.
- [29] J. Warnatz, U. Maas, and R.W. Dibble. *Combustion - Physical and Chemical Fundamentals, Modeling and Simulation, Experiments, Pollutant Formation*. Springer-Verlag Berlin Heidelberg, 4th edition, 2006.
- [30] Wikipedia. Isomer. Website, July 2009. [http://en.wikipedia.org/wiki/Isomer#cite\\_note-0](http://en.wikipedia.org/wiki/Isomer#cite_note-0).
- [31] A. Wimmer. *Thermodynamik des Verbrennungsmotors*. Institut für Verbrennungskraftmaschinen und Thermodynamik, 2004.
- [32] Y. Yacoub, R. Bata, and M. Gautam. The performance and emission characteristics of C<sub>1</sub> to C<sub>5</sub> alcohol-gasoline blends with matched oxygen content in a single-cylinder spark ignition. *Proceedings of the Institution of Mechanical Engineers, Part A: Journal of Power and Energy*, 212(5):363–379, 1998.



## List of Symbols

<i>ABDC</i>	After bottom dead centre
<i>AKI</i>	Anti knock index: $(RON + MON)/2$
<i>ATDC</i>	After top dead centre
<i>BBDC</i>	Before bottom dead centre
<i>BMON</i>	Blending motor octane number
<i>BON</i>	Blending octane number
<i>BPCR</i>	Best point compression ratio
<i>BRON</i>	Blending research octane number
<i>CA</i>	Crank angle
<i>CA50</i>	Crank angle degree where 50% fraction in mass is burnt
<i>CAD</i>	Crank angle degree
<i>CFR</i>	Cooperative fuel research engine
<i>CI</i>	Combustion interval – bulk burn duration from spark timing to 10% MFB
<i>CV</i>	Calorific value
<i>DAQ</i>	Data acquisition
<i>DON</i>	Determined octane number
<i>ECU</i>	Electrical control unit
<i>EGR</i>	Exhaust gas recirculation
<i>EVC</i>	Exhaust valve closing
<i>EVO</i>	Exhaust valve opening

<i>ID</i>	Ignition delay – bulk burn duration from spark timing to 10% MFB
<i>IMEP</i>	Indicated mean effective pressure
<i>IMPO</i>	Integral of Modulus of Pressure Oscillation
<i>IVC</i>	Inlet valve closing
<i>IVO</i>	Inlet valve opening
<i>K.I.</i>	Knock intensity
<i>KLCR</i>	Knock limiting compression ratio
<i>LHV</i>	Lower heating value
<i>LHV<sub>m</sub></i>	Lower heating value of stoichiometric air/fuel mixture
<i>MAP</i>	Manifold absolute pressure
<i>MAPO</i>	Maximum amplitude of pressure oscillation
<i>MR</i>	Micrometer reading
<i>O.N.</i>	Octane number
<i>PRF</i>	Primary reference fuels
<i>RON</i>	Research octane number
<i>S/B</i>	Stroke to bore ratio
<i>ST</i>	Spark timing
<i>UC</i>	University of California
<i>Carbob</i>	California before oxygenate blend
<i>f<sub>s</sub></i>	Sampling frequency
<i>m<sub>fb</sub></i>	Mass fraction burnt
<i>n</i>	Polytropic index
<i>rpm</i>	Revolutions per minute
<i>W<sub>i</sub></i>	Indicated work
<i>η<sub>i</sub></i>	Indicated efficiency

$\eta_m$	Mechanical efficiency
$\gamma$	Ratio of specific heat capacities
$\lambda$	Air/fuel ratio
$\tau$	Ignition time delay





# A. Calculations

## Stoichiometric Air Requirement

The stoichiometric air requirement is defined as

$$Air_{st} = \frac{m_{Air,st}}{m_{Fuel}} = \frac{m_{O_2,st}}{m_{Fuel} \xi_{O_2,Air}} . \quad (A.1)$$

whereas the mass fraction of  $O_2$  in air is given by

$$\xi_{O_2,Air} = \frac{m_{O_2,Air}}{m_{Air}} = \frac{n_{O_2,Air} M_{O_2}}{n_{Air} M_{Air}} \quad (A.2)$$

with  $m$  denoting the mass,  $M$  denoting the molar mass and  $n$  the number of moles of each molecule. The denominator of equation A.2 , the mass of air, can also be expressed as

$$m_{Air} = n_{Air} M_{Air} = n_{O_2,Air} M_{O_2} + n_{N_2,Air} M_{N_2} . \quad (A.3)$$

Combining equation A.2 with equation A.3 and assuming the composition of the air to be of 79% nitrogen and 21% oxygen leads to

$$\xi_{O_2,Air} = \frac{1}{1 + \frac{n_{N_2,Air} M_{N_2}}{n_{O_2,Air} M_{O_2}}} = \frac{1}{1 + \frac{0.79 \cdot 28}{0.21 \cdot 32}} = 0.233 \frac{kg O_2}{kg Air} . \quad (A.4)$$

For a hydrocarbon fuel with the chemical formula  $C_x H_y O_z$  the stoichiometric air requirement can be derived from the chemical reaction



whereas the required oxygen for stoichiometric combustion is

$$n_{O_2,st} = (x + \frac{y}{4} - \frac{z}{2}) O_2 \frac{kmol O_2}{kmol Fuel} . \quad (A.6)$$

By combining equation A.1 with equation A.6 and A.4 the stoichiometric air requirement can finally be calculated as

$$Air_{st} = \frac{1}{\xi_{O_2,Air}} \frac{n_{O_2,st}}{n_{Fuel}} \frac{M_{O_2}}{M_{Fuel}} \frac{kg Air}{kg Fuel} \quad (A.7)$$

whereas the molar mass of the fuel is defined as the sum of the moles multiplied by the molar mass of each molecule (see A.10).

## Properties of Air/Fuel Mixtures

### Gas Constant of Mixtures

The gas constant of a mixture is defined by the sum of mass fraction multiplied by the gas constant of each component.

$$R_{\text{Mixture}} = \sum_{i=1}^n \xi_i R_i = \xi_{\text{Air}} R_{\text{Air}} + \xi_{\text{Fuel}} R_{\text{Fuel}} \quad (\text{A.8})$$

The mass fraction of the fuel can be calculated with

$$\xi_{\text{Fuel}} = \frac{m_{\text{Fuel}}}{m_{\text{Fuel}} + m_{\text{Air}}} = \frac{1}{1 + \frac{m_{\text{Air}}}{m_{\text{Fuel}}}} = \frac{1}{1 + \lambda \text{Air}_{\text{st}}} \xi_{\text{Air}} = 1 - \xi_{\text{Air}} \quad (\text{A.9})$$

The molar mass of a mixture is defined as the sum of the moles multiplied by the molar mass of each molecule

$$M_i = \sum_{i=1}^n n_i M_i \quad (\text{A.10})$$

and the gas constant of a molecule derives from the universal gas constant  $R$  and the molar mass of the molecule

$$R_i = \frac{R}{M} \quad (\text{A.11})$$

Now all variables in order to solve equation A.8 are defined and the gas constant of a air/fuel mixture can be calculated.

### Lower Heating Value

For stoichiometric air/fuel mixtures the lower heating value ( $LHV_{\text{Mixture}}$ ) is defined by

$$LHV_{\text{Mixture}} = \frac{m_{\text{Fuel}} LHV}{V_{\text{Mixture}}} \quad (\text{A.12})$$

whereas  $m_{\text{Fuel}}$  is the mass of fuel,  $LHV$  the lower heating value of the fuel and  $V_{\text{Mixture}}$  the volume of the mixture in the cylinder before ignition. For port-fuel-injected engines the intake of an air/fuel mixture has to be considered, hence

$$V_{\text{Mixture}} = \frac{m_{\text{Mixture}}}{\rho_{\text{Mixture}}} = \frac{m_{\text{Fuel}} + m_{\text{Air}}}{\rho_{\text{Mixture}}} \quad (\text{A.13})$$

Combining the two above equations yields to

$$LHV_{\text{Mixture}} = \frac{m_{\text{Fuel}} \rho_{\text{Mixture}} LHV}{m_{\text{Mixture}}} = \frac{\rho_{\text{Mixture}} LHV}{1 + \frac{m_{\text{Air}}}{m_{\text{Fuel}}}} \quad (\text{A.14})$$

By expanding  $m_{\text{Air}}/m_{\text{Fuel}}$  by the term  $\text{Air}_{\text{st}}/\text{Air}_{\text{st}}$

$$\frac{m_{\text{Air}}}{m_{\text{Fuel}}} = \frac{m_{\text{Air}}}{m_{\text{Fuel}}} \frac{\text{Air}_{\text{st}}}{\text{Air}_{\text{st}}} = \lambda \text{Air}_{\text{st}} \quad (\text{A.15})$$

simplifies the equation for the calorific value to

$$LHV_{\text{Mixture}} = \frac{\rho_{\text{Mixture}} LHV}{1 + \lambda Air_{\text{st}}} \quad (\text{A.16})$$

The only unknown in the above equation is the specific gravity of the mixture. From the ideal gas law  $pV=RT$ , whereas  $v=1/\rho$ , the specific gravity of the mixtures is

$$\rho_{\text{Mixture}} = \frac{p_{\text{Mixture}}}{R_{\text{Mixture}} T_{\text{Mixture}}}. \quad (\text{A.17})$$

whereas the gas constant of the mixture is defined in equation A.8.

## Heat Release Rate

The heat release is equal to the amount of energy that had to be added to the cylinder content in order to produce the observed pressure variations. A single zone model is applied what assumes fully mixed products and reactants. By applying the first law of thermodynamics to a control volume in which there is no mass transfer ( $\sum h_i dm_i = 0$ ) then the heat release rate is given by:

$$\partial Q_{\text{hr}} = dU + \partial W + \partial Q_{\text{ht}} \quad (\text{A.18})$$

where  $dU$  denotes the change in internal energy,  $\partial W$  the work done by the piston and  $\partial Q_{\text{ht}}$  the heat transfer through the wall. The internal energy can be modeled with

$$dU = m c_v dT. \quad (\text{A.19})$$

From the equation of state ( $pV = mRT$ ) and by assuming the cylinder mass to stay constant it follows

$$m dT = \frac{1}{R} (pdV + V dp). \quad (\text{A.20})$$

Substitution of equation A.19 into equation A.20 gives:

$$dU = \frac{c_v}{R} (pdV + V dp) \quad (\text{A.21})$$

The heat release analysis considering the heat transfer through the walls is called gross heat release. Therefore a heat transfer correlation has to be employed. In this work the net heat release rate was applied which does not consider the heat transfer through the walls.

$$\frac{dQ_{\text{net}}}{d\theta} = \frac{dQ_{\text{hr}}}{d\theta} - \frac{dQ_{\text{ht}}}{d\theta} = dU + dW \quad (\text{A.22})$$

With the work done by the piston equal to  $dW = pdV$  and by substituting equation A.21 into equation A.22 the net heat release on an incremental basis is:

$$\frac{dQ_{\text{net}}}{d\theta} = \frac{c_v}{R} (pdV + V dp) + p \frac{dV}{d\theta} \quad (\text{A.23})$$

The term  $dp/d\theta$  has been recorded in the experiments. By assuming semi-perfect gas behaviour with  $c_p/c_v = \gamma$  and  $R = c_p - c_v$  equation A.23 can be written as:

$$\frac{dQ_{\text{net}}}{d\theta} = \frac{\gamma}{\gamma - 1} p \frac{dV}{d\theta} + \frac{1}{1 - \gamma} V \frac{dp}{d\theta} \quad (\text{A.24})$$

### Volume of Combustion Chamber

The cylinder volume at every crank angle degree can be calculated from the geometry of the engine. The compression ratio of the engine is variable and the clearance volume changes with the compression ratio. It can be calculated by:

$$V_C = \frac{B^2 \pi}{4} (DH + MR) * 0.254 \quad (\text{A.25})$$

with  $DH = 0.273$  in the deck height,  $MR$  the micrometer reading equal to the height of the cylinder head and  $B$  the bore of the piston. The factor 0.254 is to convert unit inches to unit meter. The actual volume of the cylinder is then calculated by

$$V = V_C + \left[ R + l - (R \cos(\theta) + \sqrt{l^2 - (R \sin(\theta))^2}) \right] \frac{B^2 \pi}{4} \quad (\text{A.26})$$

where  $B = 82.65 \text{ mm}$  (Cylinder Bore)  
 $S = 114.3 \text{ mm}$  (Stroke)  
 $R = 82.65 \text{ mm}$  Crank throw (Stroke/2)  
 $l = 254 \text{ mm}$  Con-rod length  
 $V_C$  Clearance Volume at TDC

## B. Chemical Properties of Alcohols

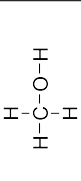




Name	Methanol	Ethanol	1-Propanol	1-Butanol	1-Pentanol	Gasoline
Chemical Formula	CH <sub>3</sub> OH	C <sub>2</sub> H <sub>5</sub> OH	C <sub>3</sub> H <sub>7</sub> OH	C <sub>4</sub> H <sub>9</sub> OH	C <sub>5</sub> H <sub>11</sub> OH	
Chemical structure						
CAS Registry Number	67-56-1	64-17-5	71-23-8	71-36-3	71-41-0	
Molecular mass	32.0419	46.0684	60.0950	74.1216	88.1482	111.21 (UTG96)
Density (20 °C, 1 bar) [kg/m <sup>3</sup> ]	791.32	789.24	803.20	809.80	813.3	≈ 0.739
Heat capacity $c_P$ [J/molK]	80.225	112.4	144.4	x	x	x
Lower heating value [MJ/kg]	19.9	26.8	30.7	33.1	34.8	42-44
Lower heating value [MJ/l]	15.8	21.1	24.7	26.7	28.3	≈ 32.3
Oxygen content [wt%]	49.9	34.7	26.6	21.6	18.2	0
Boiling point [K (°C)]	337.75 (64.6)	351.44 (78.29)	370.35 (97.20)	390.88 (117.73)	411.13 (137.98)	34 - 207
Flash point [°C]	12	13	23	37	33	
Autoignition Temperature [°C]	464	425	412	343	300	
Reid vapor pressure [kPa]	32.4	19.3	9	18.6		61.4
Heat of vaporization [kJ/kg]	1098.63	837.86	688.85	584.19	503.68	348.88
Heat of vaporization at Boiling point [kJ/mol]	35.91	38.56	41.44	43.29	44.36	
Stoichiometric air/fuel ratio	6.46	8.98	10.33	11.17	11.74	14.70
Stoich. Flame speed [cm/s]	43	41			34	
RON	112	111		94		≈ 92-98
MON		91	92	92		≈ 80-90

Table B.1.: Physical and chemical properties of alcohols and non-oxygenated gasoline (UTG96) [6], [13], [16], [18], [32].

## C. Determination of Knock Limiting Compression Ratio

